ИТМО

А.А. Старовойтов, А.А. Матюшкина

LABORATORY ASSIGNMENTS FOR THE COURSE «NONLINEAR OPTICS»

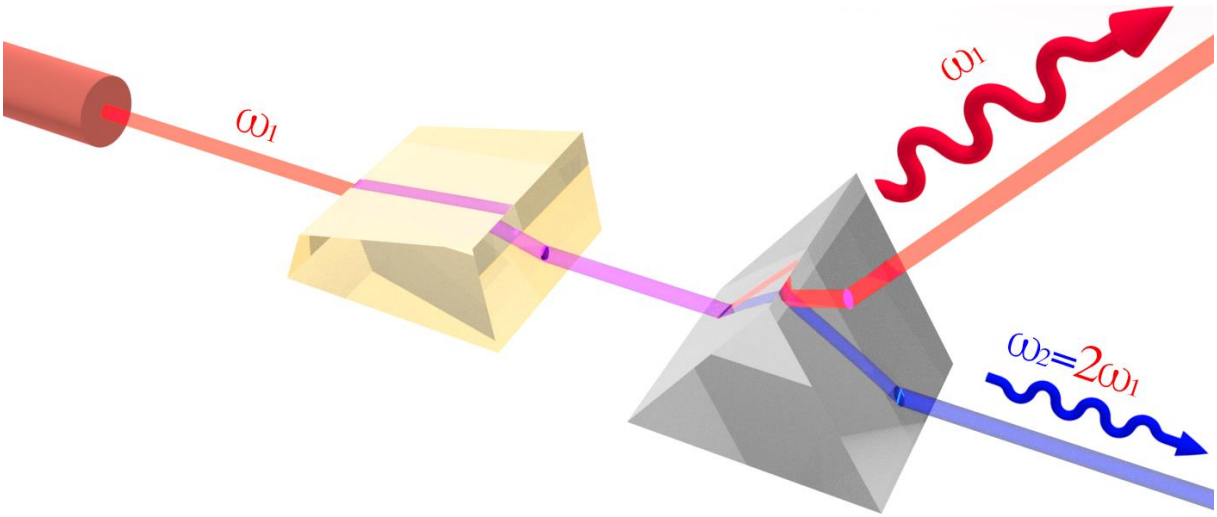

Санкт-Петербург
2023

МИНИСТЕРСТВО НАУКИ И ВЫСШЕГО ОБРАЗОВАНИЯ РОССИЙСКОЙ ФЕДЕРАЦИИ

УНИВЕРСИТЕТ ИТМО

А.А. Старовойтов, А.А. Матюшкина

LABORATORY ASSIGNMENTS FOR THE COURSE «NONLINEAR OPTICS»

ПРАКТИКУМ

РЕКОМЕНДОВАНО К ИСПОЛЬЗОВАНИЮ В УНИВЕРСИТЕТЕ ИТМО
по направлению подготовки 12.04.03 Фотоника и оптоинформатика
в качестве практикума для реализации основных профессиональных образовательных программ высшего образования магистратуры

Санкт-Петербург
2023

Старовойтов А.А., Матюшкина А.А., Laboratory assignments for the course «Nonlinear Optics» – СПб: Университет ИТМО, 2023. – 68 с.

Рецензент(ы):
Гладских Игорь Аркадьевич, кандидат физико-математических наук, старший научный сотрудник центра "Информационные оптические технологии", Университета ИТМО.

Предлагаемый лабораторный практикум к дисциплине "Nonlinear Optics" познакомит студентов с наиболее известными нелинейно-оптическими явлениями, а также даст навыки физического эксперимента и опыт работы с мощным лазерным комплексом. Реализация обучения проходит на оборудовании лаборатории «Фотофизика поверхности» международного научно-образовательного центра "Физика наноструктур" для магистрантов направления подготовки "Фотоника и оптоинформатика".

Университет ИТМО – ведущий вуз России в области информационных и фотонных технологий, один из немногих российских вузов, получивших в 2009 году статус национального исследовательского университета. С 2013 года Университет ИТМО – участник программы повышения конкурентоспособности российских университетов среди ведущих мировых научно-образовательных центров, известной как проект «5 в 100». Цель Университета ИТМО – становление исследовательского университета мирового уровня, предпринимательского по типу, ориентированного на интернационализацию всех направлений деятельности.

CONTENT

INTRODUCTION

The emergence of "nonlinear optics" as a branch of physics resulted from the invention of optical quantum generators (lasers). Before the invention of lasers, experiments used optical radiation, in which electric field strength was negligible compared to intraatomic and intramolecular fields. The intensity of modern high-power lasers reaches 10^{20} W/cm^2 or more, which is comparable to the electric field strength inside atoms. The use of laser light sources with such intensity leads to new nonlinear optical effects [1]. The effects depending on the radiation intensity are called nonlinear optical effects, and the section of physical optics that studies them is called nonlinear optics.

The laboratory assignments presented in this manual use the equipment of the "Surface Photophysics" laboratory run by Professor, Doctor of Physical and Mathematical Sciences Tigran Armenakovich Vartanyan.

The "Surface Photophysics" laboratory has existed as part of the International Research and Educational Center for Physics of Nanostructures since its foundation in 2006. Prior to that date, all its members were employed at the S. I. Vavilov State Optical Institute, where more than 60 years ago the Corresponding Member of the Russian Academy of Sciences Alexei Mikhailovich Bonch-Bruevich founded a scientific school and the laboratory team to study the interaction of high-power laser radiation with matter. The scientific school of A.M. Bonch-Bruevich received the official status of a leading scientific school following the results of the first competition organized in 1996 according to the Decree of the Government of the Russian Federation, and since then it repeatedly confirmed this status.

The laboratory team was closely involved in the development of laser physics in our country. As early as in 1963, the laboratory staff received the first copyright certificates for inventions in the field of laser technology. The review of "Multiphoton Processes" by A.M. Bonch-Bruevich and V.A. Khorovod published in the journal "Advances in physical sciences" (in Russian) in 1965, laid the foundation for this new direction in optics and has been much referred to till now. The first domestic mass-produced neodymium laser and the most powerful laser in 1960s (GSN-1) were developed by the team supervised by A.M. Bonch-Bruevich. At the same time, the laboratory started its research on the destructive effect of high-power radiation on metals and dielectrics, as well as fundamental research on reversible changes in the optical properties of various media under the action of powerful, but not damaging, laser radiation. Both directions of research were essential for multiple applications. T.K. Razumova discovered and studied the changes in the absorption spectra of the first laser material (ruby), whereas V.V. Khromov investigated the absorption spectra of atoms in the gas phase. In 1975 V.L. Komolov theoretically developed a statistical model of glass optical breakdown, for which he later received the Lenin Komsomol Prize. In 1972, the S.G. Przhibelsky's papers provided the

fundamental basis for a theoretical description of nonlinear optical phenomena in non-monochromatic fields of laser radiation.by. Further, the laboratory conducted research in many related areas.

T.K. Razumova's group studied photoinduced reversible transformations of the stereostructure of polyatomic organic molecules and carried out a series of research on the organic media generation characteristics for tunable lasers.

V.V. Khromov's group studied the dynamic Stark effect in alkali metal atoms in monochromatic and non-monochromatic radiation fields. They discovered and studied in detail the phenomenon of four-wave interaction in resonant media, which later became the basis of dynamic holography. The group was actively involved in the study of atomic collisions in intense radiation fields, which resulted in the formation of a new scientific direction - radiative collisions. At the same time, they discovered a new type of resonant medium optical clearing based on Landau-Zener type nonlinearity. Their studies included a research on the phenomena involved in the absorption of resonant radiation by an adsorption complex consisting of an atom adsorbed on the surface and nearby atoms of the substrate (photodesorption and photodiffusion) were studied. A new physical phenomenon was discovered - photoatomic emission, which consists in the photoinduced detachment of its own atoms from the metal's surface.

S.G. Przhibelsky gave a theoretical description of new processes observed during the action of non-monochromatic laser radiation on various nonlinear materials, He was the first to reveal the harmonics intraspectral correlation during nonlinear optical phenomena and started a related research. He carried out the pioneering theoretical work in the new field of radiative collisions of atoms, and predicted the echo phenomenon in half-collisions of atoms. He provided a theoretical description of the atoms photodesorption and photodiffusion over the alien and the own surfaces of elements, and developed the theoretical basis for a new method for studying submicron particles - that of fluctuation microscopy.

At present, the laboratory "Surface Photophysics" of ITMO University, with its new generation of young PhDs, is conducting intensive research on composite materials, which include nanoparticles of noble metals. An essential feature of noble metal nanoparticles is that all the conduction electrons they include participate in the vibrations under the action of external electromagnetic radiation. As a result, the collective response to an external action appears to be greater than that of other resonant systems, and a region forms near the nanoparticle where the energy density of the electromagnetic field is higher than that in the incident wave. By placing various resonant systems with a useful but relatively weak response in the near field of plasmonic nanoparticles, absorption can be significantly increased, followed by an increase in the luminescence intensity and acceleration of other processes. The composites produced are of particular interest including epitaxial semiconductor quantum dots in single-crystal gallium arsenide, which can be used in optoelectronic devices. The

laboratory also studies the composites with organic dyes, among which those forming J-aggregates. They investigate the possibility of using metal nanoparticles to study the kinetics of processes in living cells. The photonics of atomic vapors nanosized layers is being developed to improve the model of a nanosensor for non-invasive studies of biological tissues.

The laboratory assignments suggested will introduce the most well-known nonlinear optical phenomena, as well as provide students with the skills to conduct a physical experiment and gain some experience in working with a powerful laser complex. The description of the laboratory part includes the order of actions that students have to perform under the lecturer’s supervision. On the other hand, the methodological manual does not contain any formulas for processing the results obtained. This is done so that the students could independently derive the necessary solutions and use the adequate mathematical apparatus to calculate errors.

The manual is recommended to be used in the implementation of the discipline "Nonlinear Optics" for a semester course of the Master's program "Physics and technology of nanostructures". The purpose of the manual is to describe the practical work in a scientific laboratory, which is meant to consolidate the theoretical knowledge gained in the lecture course.

1 LABORATORY ASSIGNMENT "SECOND HARMONIC GENERATION"

1.1 Theoretical information

One of the most important processes in nonlinear optics is the generation of optical radiation higher harmonics, in particular, the second harmonic, which is usually abbreviated as SHG.

1.1.1 Principles of second harmonic generation (SHG)

The SHG discovery is closely related to the development of intense monochromatic radiation sources, lasers. It was made only a year after the ruby laser was produced by Theodor Maiman (USA) in 1960. In 1961, a group of scientists under Peter Franken at the University of Michigan was the first to receive radiation at the second harmonic by directing a ruby laser beam at a quartz crystal (Fig. 1.1a). Since the wavelength of the ruby laser is 694.3 nm, the second harmonic is in the near ultraviolet spectrum region (λ/2, i.e. 347.1 nm). It is worth mentioning that the SHG effect in this experiment was observed in the absence of phase matching, which caused a very low conversion coefficient to the second harmonic.

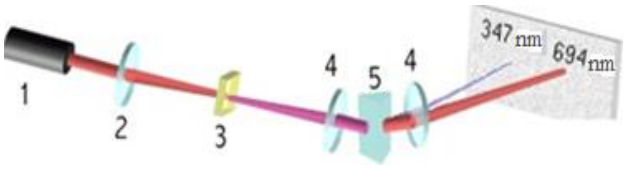

a

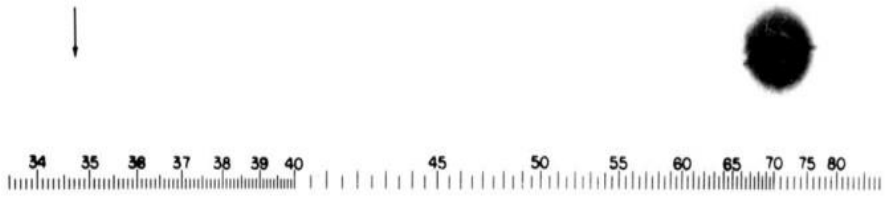

FIG. 1. A direct reproduction of the first plate in which there was an indication of second harmonic. The wavelength scale is in units of 100 A. The arrow at 3472 A indicates the small but dense image produced by the second harmonic. The image of the primary beam at 6943 A is very large due to halation.

b

Figure 1.1 – a: diagram of the Franken experiment for SHG (1 – ruby laser, 2 and 4 – converging lenses, 3 – quartz crystal, 5 – dispersive prism); b: a Figure from Franken's article in Physical Review Letters (volume 7, page 19, published 1961)

It is noteworthy that when the experiment was published in the Physical Review Letters journal, the editor mistook a faint spot (at 347 nm) on photographic paper for a speck of dirt and removed it from the publication (Fig. 1.1b).

The low conversion efficiency problem to the second harmonic was solved by Joseph Jordmain in 1962 by matching the refractive indices (n) for radiation at the fundamental and doubled frequency - the so-called phase (or wave) matching method. The method is based on choosing a certain direction in a nonlinear medium, along which the phase velocities of the exciting radiation and the second harmonic would be the same. Thus, the SHG efficiency sharply increases due to an increase in the wave interaction length.

1.1.2 Phenomenological SHG description

The generation of sum frequencies consists in the appearance in the medium of a wave with a frequency of ω_3 while the two other waves are propagating with the frequencies of ω_1 and ω_2:

$$\omega_1 + \omega_2 = \omega_3$$

If the same waves pass through the medium ($\omega_1 = \omega_2 = \omega$), we observe a special case - second harmonic generation:

$$\omega + \omega = 2\omega$$

Let us consider the reason for this effect. The interaction of an incident electromagnetic wave with a substance is described by the polarization vector **P**, which depends on the strength of the wave electric field: **P** = f(**E**). In the linear optics approximation, the polarization is linearly related to the intensity **E**:

$$\mathbf{P} = \chi^{(1)}\mathbf{E},$$

where $\chi^{(1)}$ is the linear optical susceptibility of the medium.

This approximation can be used for common light sources, which have a much lower intensity ($I \sim E^2$) compared to lasers. However, the relationship between the polarization **P** and the intensity **E** starts to differ slightly from the linear one in strong laser fields, so the function **P** = f(**E**) can be represented as a series expansion in powers of the wave electric field

$$\mathbf{P} = \chi^{(1)}\mathbf{E} + \chi^{(2)}\mathbf{EE} + \chi^{(3)}\mathbf{EEE} + \ldots$$

The first term is linear, and the others are the nonlinear components of polarization, quadratic and cubic, respectively. The ratio of each subsequent member of the series to the previous one is $\sim 1/E_{ampl}$, i.e. subsequent members of the series rapidly decrease. It should be noted that the series expansion is contingent, l since the value $\chi^{(i)}$ are tensors of (i+1) rank.

The SHG appearance is related to the quadratic term $\chi^{(2)}\mathbf{EE}$ in the expansion of the polarization **P**. If a harmonic electromagnetic wave $E = A\cdot\sin(\omega t)$ is incident on the medium, then the polarization, and, consequently, the reradiated wave, will not only contain the frequency ω, but its doubled harmonic 2ω as well:

$$P_2 = \chi^{(2)}E^2 = \chi^{(2)}\cdot A^2\cdot\sin^2(\omega t) = 0.5\cdot\chi^{(2)}\cdot A^2\cdot(1-\cos(2\omega t)) =$$

$$= 0.5 \cdot \chi^{(2)} \cdot A^2 - 0.5 \cdot \chi^{(2)} \cdot A^2 \cdot \cos(2\omega t)$$

The second term in the resulting expression describes the field re-radiated by the electron at a frequency of 2ω, i.e. the second harmonic of the falling frequency. For this term to be present, it is also important that the coefficient $\chi^{(2)}$ should be different from zero, which is the case in anisotropic media that do not have a center of symmetry. Thus, isotropic crystals or crystals with a cubic system (crystal lattice) are not suitable for SHG.

1.1.3 Phase matching condition for SHG

The generation of radiation at the sum (or difference) frequency is the most efficient if a wave with a frequency ω_3 coming to a given volume element from the previous elements is in the required phase with the radiation at the same frequency, which is generated in this volume element. Thus, the intensity of the radiation generated increases by several orders of magnitude due to interference processes along the entire length of the nonlinear medium. Such a phase relation can be observed in the case of the wave vectors equality:

$$\mathbf{k}_1 + \mathbf{k}_2 = \mathbf{k}_3$$

This expression is referred to as the condition of spatial phase (wave) matching in vector form.

As mentioned above, second harmonic generation is a special case of frequency summation when $\omega_1 = \omega_2 = \omega$, thus:

$$\mathbf{k}_\omega + \mathbf{k}_\omega = \mathbf{k}_{2\omega},$$

The condition of collinear phase matching, when the wave vectors lie on one straight line, can be written in terms of the wave vectors modulus:

$$k_\omega + k_\omega = k_{2\omega},$$

where $k = 2\pi n/\lambda$ is the wave number. Thus, the equality of the refractive indices follows: $n_\omega + n_\omega = 2n_{2\omega}$, since $\lambda_\omega = 2\lambda_{2\omega}$. That is, to implement phase matching in a nonlinear medium, it is necessary that:

$$n_\omega = n_{2\omega}$$

In optical media with normal dispersion, such an equality is impossible since the refractive index increases with increasing frequency $n(\omega)$. However, in birefringent crystals that are anisotropic, it is possible to choose a propagation direction, for which the refractive index of the ordinary ray of the fundamental frequency $n_o(\omega)$ is equal to the refractive index of the extraordinary ray of the second harmonic $n_e(2\omega)$. Figure 1.2 schematically shows a section of refractive index surfaces (refractive index indicatrix) for a negative uniaxial crystal, i.e. for which at a given fixed frequency $n_e < n_o$ (the most common case in practice). In such crystals, the direction of light propagation can be found, along which the exponents will be equal ($n_o(\omega) = n_e(2\omega)$). The direction to the intersection point, forming the angle θ_c, $\pi+\theta_c$, $2\pi-\theta_c$, $\pi-2\theta_c$ with the optical axis of the crystal, is the direction of phase matching for the excitation wave and the second harmonic. Angle θ_c in fig. 1.2 is referred to as the matching angle. The SHG intensity in this direction is several orders of magnitude higher than in other directions. Due

to the axial symmetry, the directions of phase matching form a conical surface with an angle at the apex equal to $2\theta_c$.

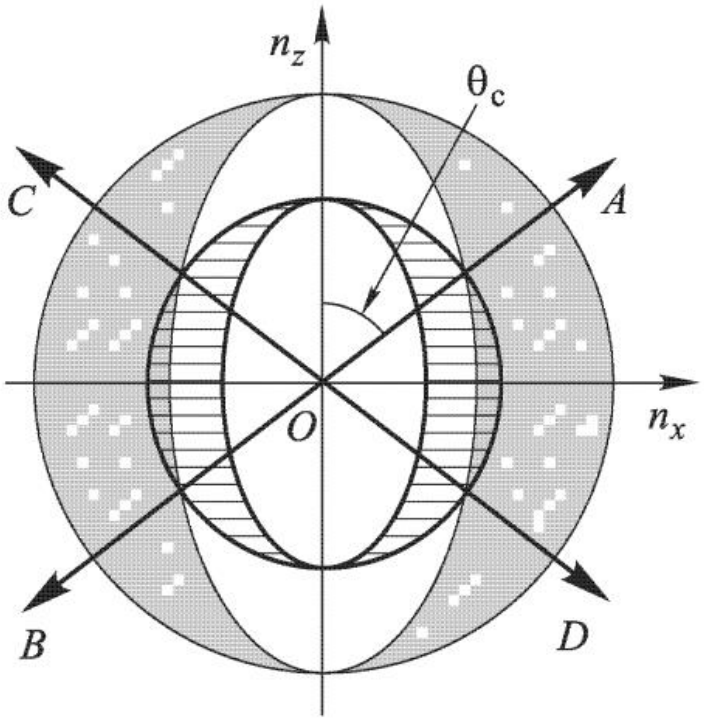

Figure 1.2 – The refractive index indicatrices sections of a negative uniaxial crystal for the fundamental frequency (thick lines) and the second harmonic (thin lines)

Thus, by directing the exciting radiation as an ordinary wave at an angle θ_c, it is possible to obtain effective SHG in a nonlinear crystal as an extraordinary wave along the same direction. Such an interaction is classified as type I: oo-e, because two linearly polarized waves of the main radiation (ordinary in a given crystal) generate an extraordinary wave of doubled frequency, which has an orthogonal linear polarization.

SHG is possible in the interaction of the fundamental radiation ordinary and extraordinary waves with an extraordinary wave of doubled frequency, i.e. oe-e interaction (or type II), for many nonlinear optical crystals.

On the other hand, in real systems, the matching direction has a certain small angular width: $\theta_c \pm \alpha$, where α is the detuning angle, which is one minute or less. That is, phase matching is not implemented and SHG is not observed at incidence angles greater than $(\theta_c + \alpha)$ and less than $(\theta_c - \alpha)$.

In addition, the phase-matching condition imposes a restriction on the monochromaticity of the interacting waves, with the width of the laser emission line usually not exceeding several angstroms. This implies some requirements for laser radiation at the fundamental frequency - the divergence is to be less than the angular matching width, and its monochromaticity cannot exceed the frequency width. Otherwise, less than the whole laser beam power will be involved in SHG.

The radiation intensity at the doubled frequency under the condition of phase matching is equal to:

$$I_{2\omega} = a \cdot (I_{\omega})^2 \cdot l^2,$$

where the coefficient $a(\chi^{(2)}, \omega_i, n_i)$ characterizes the "quality" of the nonlinear crystal. It depends on the nonlinear polarizability of the medium $\chi^{(2)}$, on the frequencies of the interacting waves ω_i and on the refractive indices of the medium n_i at those frequencies.

It is noteworthy that under certain conditions (for example, when the crystal temperature changes), the spherical surface of the refractive index for an ordinary fundamental wave only touches the ellipsoidal surface of an extraordinary wave at a doubled frequency, but does not cross it. Then the angle θ_c is 90° (Fig. 1.3), and phase matching becomes less dependent on the angle.

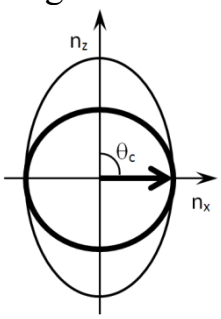

Figure 1.3 – Phase matching at $\theta_c = 90°$

1.2 Questions

1. Which of the medium polarization terms is responsible for the second harmonic generation?
2. What is the phase matching condition?
3. What is a negative uniaxial crystal?
4. What are the parameters of the angular width of the phase-matching direction?
5. How does the second harmonic intensity change in the case of phase matching with increasing crystal length?

1.3 Laboratory part

1. After the lecturer's instruction, turn on the laser complex and set up the equipment for second harmonic generation according to the brief guide given in Chapter 5.
2. Use a filter holder to place a light filter, which reduces the energy to values in the range of 50 - 100 mJ, in the path of the laser beam. Refer to the specifications for the energy of the output radiation of the second harmonic. The light filter is to be chosen using the optical glass catalog. Then measure the transmission of the light filter at the desired wavelength using the SF-56 spectrophotometer, according to the instructions and/or the lecturer's advice.

3. Install the energy meter PE50BF-C + Nova after the light filter. Turn on the device and set it to measure the energy at a wavelength of 532 nm, according to the instructions and/or the lecturer's advice.

4. Measure the dependence of the radiation energy of the second harmonic on the supposed position of the crystal, using the adjusting screw 31 (see Fig. 5.3) After completing the measurements, turn off the laser complex.

5. Enter data in Table 1.1.

Table 1.1 – Experimental data for laboratory assignment №1

β	**E_{av}**	**T_f**	**E_{exp}**
deg.	**mJ**	**%**	**mJ**
0			
90			
180			
…			

β – screw angle 31;

E_{av} {Avg} – average value of the measured energy, according to the Nova meter;

T_f – filter transmittance coefficient at a specified wavelength, measured on an SF-56 spectrophotometer;

E_{exp} – average value of the laser radiation pulse energy, taking into account the transmission of the light filter.

6. Plot a graph of the dependence of the energy of the second harmonic on the angular detuning of the crystal E_{exp} (α), based on the fact that one full turn of the 31 (360^o) adjusting screw turns the crystal by 24 arc seconds.

7. From the data obtained, find the width of the angular matching 2α.

8. Based on the data obtained, conduct a comparative analysis of experimental results and specification, and give their interpretation.

2 LABORATORY ASSIGNMENT "THIRD HARMONIC GENERATION"

2.1 Theoretical information

The generation of the second harmonic is impossible in the electric dipole approximation in crystals with an inversion center, although it can be induced by applying a constant external electric field. On the other hand, the third harmonic generation process is always possible. The theory of the third harmonic generation in the approximation of a given pump field does not differ from that of the second harmonic generation, however, instead of the quadratic polarization $P_2(2\omega)$, the formula will include the cubic polarization:

$$P_3(3\omega) = \chi^{(3)}\mathbf{EEE}$$

Since the $\chi^{(3)}$ value is usually small compared to $\chi^{(2)}$, and the intensity of laser radiation in crystals is often limited by the beginning of optical damage, the conversion efficiency in this third-order nonlinear optical process is low. Besides, it is more difficult to meet the condition of phase matching. Therefore, the process of direct third harmonic generation is not much used in practice.

2.1.1 Third harmonic generation in crystals

Direct generation of the third harmonic in a crystal with cubic nonlinearity was obtained in 1963 by the Terhune and his team. At present, the maximum direct conversion coefficient value of fundamental frequency energy into the third harmonic is about 10^{-6}. This value was obtained in a focused laser beam with Q-switching, going in the direction of the phase velocities matching. It is important that the field intensity at the focus is so strong that it can destroy almost any crystal. Therefore, when the third harmonic generation was observed, the laser beam intensity was decreased to a value a little below the critical one. The crystal destruction in a laser beam can occur because of the energy absorption by impurities, multiphoton absorption, or excitation of medium oscillations resulting from stimulated Raman scattering or stimulated Mandelstam-Brillouin scattering. In this case, the instantaneous release of heat in a small volume forms a shock wave.

However, it is possible to produce an efficient third-harmonic generator using two non-linear crystals placed next to each other. The first one generates the second harmonic. The transmitted fundamental radiation and the second harmonic radiation then interact in the second crystal and provide at the output the third harmonic radiation, which is obtained by generating the sum frequency. For both processes, it is possible to meet the condition of phase matching using matching of the first or the second type.

At a sufficiently high intensity of the fundamental radiation, the total output of the third harmonic can be quite high. Commercial samples of such devices have conversion factors to the third harmonic reaching 20%. Moreover, the

efficiency reaches 70% in high-power laser systems designed for controlled thermonuclear fusion, in the systems with thoroughly formed beams.

Overall, this two-stage generation process of the third harmonic can be implemented in a single crystal. However, except for some special cases, it is not possible to obtain matching for the second harmonic generation and sum frequency generation processes, simultaneously. Therefore, the overall conversion efficiency cannot be large.

2.1.2 Third harmonic generation in gases

The third harmonic generation is possible in gases. It may seem that, due to the much lower density of atoms or molecules in a gas compared to liquids and solids, the cubic nonlinear susceptibility of gaseous media would be much smaller than the cubic susceptibilities of liquids and solids, and that the efficiency of the third harmonic generation process in gases will be so low that this process would have no practical value. As shown by Miles and Harris, this assumption appears to be wrong. The fact is that the $\chi^{(3)}$ value increases at resonance. Much narrower transition lines in gases make it possible to obtain much greater nonlinearity near resonances, especially near those with large transition matrix elements. Besides, the maximum permissible intensity of laser radiation in gases is several orders of magnitude higher than in condensed media (it exceeds several gigawatts per square centimeter in gases, and it is several hundred megawatts per square centimeter in solids). As a result, although the $\chi^{(3)}$ is small, the nonlinear polarization P_3 induced by a high-intensity laser field can become comparable to the polarization P_2, which is induced in a solid by a moderate-intensity laser.

The possibility of the so-called direct (i.e.,conversion from the fundamental frequency directly to 3ω) generation of the third harmonic in gases was shown in the work of Miles and Harris who used sodium vapor as an example. To obtain a high conversion efficiency, in addition to a resonant increase in the susceptibility and a sufficiently high intensity of the pump wave, it is necessary to ensure that collinear phase matching condition $n(\omega) = n(3\omega)$ is met for the third harmonic generation process. Since the gas medium is isotropic, the conventional method of obtaining phase matching using the birefringence of the medium is not applicable here. In a gaseous medium in general, it does not appear to be always possible to fulfill the phase-matching condition for the process of generating the third harmonic and optical frequency mixing. However, when there is an area of anomalous dispersion between the frequencies ω and 3ω, matching can be achieved by using a buffer gas to compensate for the difference in refractive indices at frequencies ω and 3ω. When the frequency ω is lower, and the frequency 3ω is higher than the strong transition $s \rightarrow p$ in the spectrum of an alkali metal atom, then $n_s(\omega) > n_s(3\omega)$ is observed in pure metal vapors due to anomalous dispersion. If an inert gas (for example, xenon) with

normal dispersion $n_x(\omega) < n_x(3\omega)$ is mixed with the medium, then it is possible to meet the phase-matching condition by selecting its density if

$$n_s(\omega) + n_x(\omega) < n_s(\omega) + n_x(3\omega).$$

Using gaseous media for nonlinear optical mixing has a number of important advantages:

1. It is easy to obtain a homogeneous medium with a length more than 10 cm.
2. Since the medium is isotropic, there is no drift problem. Therefore, focusing can be optimized to increase the conversion efficiency.
3. Besides the high threshold for pointing optical inhomogeneities, the gaseous medium is able to self-heal. Except in some special cases, no permanent charge is formed in the medium due to laser-induced ionization and dissociation.
4. Atomic vapors are transparent to radiation at almost all frequencies below the ionization level, except for some discrete absorption lines. Besides, these vapors are the only non-linear medium that can be used in the far ultraviolet and soft X-ray ranges.

The gas medium may seem to be ideal for generating the third harmonic, especially in the ultraviolet range. Presumably, a high conversion efficiency could be obtained using a high-intensity laser and a sufficiently long gas cell. Unfortunately, there are many factors that often hinder its efficiency as they limit the amount of laser light that can be used:

1. Linear absorption at frequencies ω and 3ω causes a decrease in efficiency. The resonant increase of $\chi^{(3)}$ is simultaneous to an increase in linear absorption, although in a different proportion.
2. Two- and multi-photon absorption can play an important role in limiting conversion efficiency when high-intensity laser beams are used.
3. The populations redistribution due to the radiation absorption can lead to a phase mismatch in the process of optical frequency mixing.
4. Phase mismatch can also result from some other mechanisms of laser-induced refractive index change.
5. The process of optical mixing can be interrupted by a laser-induced medium breakdown.

The effect of all the above factors is rapidly enhanced as ω and 3ω approach resonance. Usually, it is the third factor on the list that is the most restrictive, and the fifth one can easily occur when using long laser pulses.

The third harmonic generation in gases has been experimentally observed and amply discussed. For example, matching generation of the third harmonic at a wavelength of 354.7 nm with a 10% conversion factor was observed using 30 picosecond pulses of a Nd:YAG laser with a 300 MW power, which was optimally focused into a spot with a 10^{-3} cm^2 cross-section into a cell 50 cm long with a mixture of Rb (3 Torr): Xe (2000 Torr).

2.1.3 Sum Frequency Generation (SFG)

The wave interaction in a nonlinear medium results in their mixing, and thus, waves are generated at sum and difference frequencies. Sum frequency generation is one of three nonlinear optical effects discovered at the dawn of nonlinear optics. With the development of tunable lasers, this process has become one of the most useful non-linear optical effects, since it produces wavelength-tunable radiation in the short-wavelength range.

In 1962, Bass et al. first observed sum frequency generation in the optical range in a triglycine sulfate crystal. In their experiment, two ruby lasers were used as sources of initial waves, the generation wavelengths of which were separated from each other by 1 nm. At the output, as shown by the spectrograph, three lines were observed near 347 nm. The sidelines had to do with the generation of second-harmonic waves of the pump radiation, and the middle line had to do with the generation of the sum frequency by two laser beams.

The physical interpretation of the sum frequency generation phenomenon lies in the interaction of waves with frequencies ω_1 and ω_2, which leads to the generation of nonlinear polarization $P^{(2)}(\omega_3 = \omega_1 + \omega_2)$ in the crystal. Polarization, which is a superposition of two oscillating dipoles contributions, serves as a source of radiation at a frequency $\omega_3 = \omega_1 + \omega_2$. In general, sum frequency radiation can occur in all directions. The radiation field depends on the phase-correlated spatial distribution $P^{(2)}(\omega_3)$. By choosing the geometry of the experiment, or rather, by implementing the phase-matching condition, it is possible to create directed radiation with a small divergence. For efficient energy transfer from pump waves at frequencies ω_1 and ω_2 to the wave ω_3 generated in the sum frequency process, the conditions of energy conservation ($\omega_3 = \omega_1 + \omega_2$) and momentum ($\mathbf{k_3} = \mathbf{k_1} + \mathbf{k_2}$) must be met simultaneously. If the wave interaction length l is finite, then it is enough to meet the momentum conservation condition with an uncertainty of the $1/l$ order. Thus, the radiation field will have an amplitude-limited peak in the matching direction with an angular width corresponding to $\Delta k \sim 1/l$. The absorption in the medium can limit the interaction length and broaden the peak of phase matching. In the general case, the generation of the sum frequency in the medium volume (when this process is possible, and the condition of phase matching is met) dominates over the surface contribution. In the reflected wave, where there is no phase matching, the contribution of the surface layer with a thickness of the $\lambda/2\pi$ order can be noticeable. The approach described above makes it possible to provide a qualitative description of the sum frequency generation.

2.1.4 Phase matching for SFG

Let us consider a general case of meeting phase-matching conditions for the SFG using the example of a negative uniaxial crystal. Unlike SHG (section 1.1.3), we will refer to wave vector surfaces whose configuration is similar to the refractive index surfaces in the above crystal. Figure 2.1 shows the surface sections of wave vectors by the XZ plane, when the Z axis is parallel to the

optical axis C. Let linearly polarized radiation with frequencies ω_1 and ω_2 propagate in the crystal as ordinary waves. To meet the matching condition in a negative crystal, the total wave ω_3 must be extraordinary, i.e. linearly polarized, with the vector $\mathbf{E}_3$ lying in the plane passing through the axis C and the vectors $\mathbf{k}_1$ and $\mathbf{k}_2$. This is referred to the ***ooe*** interaction (type I).

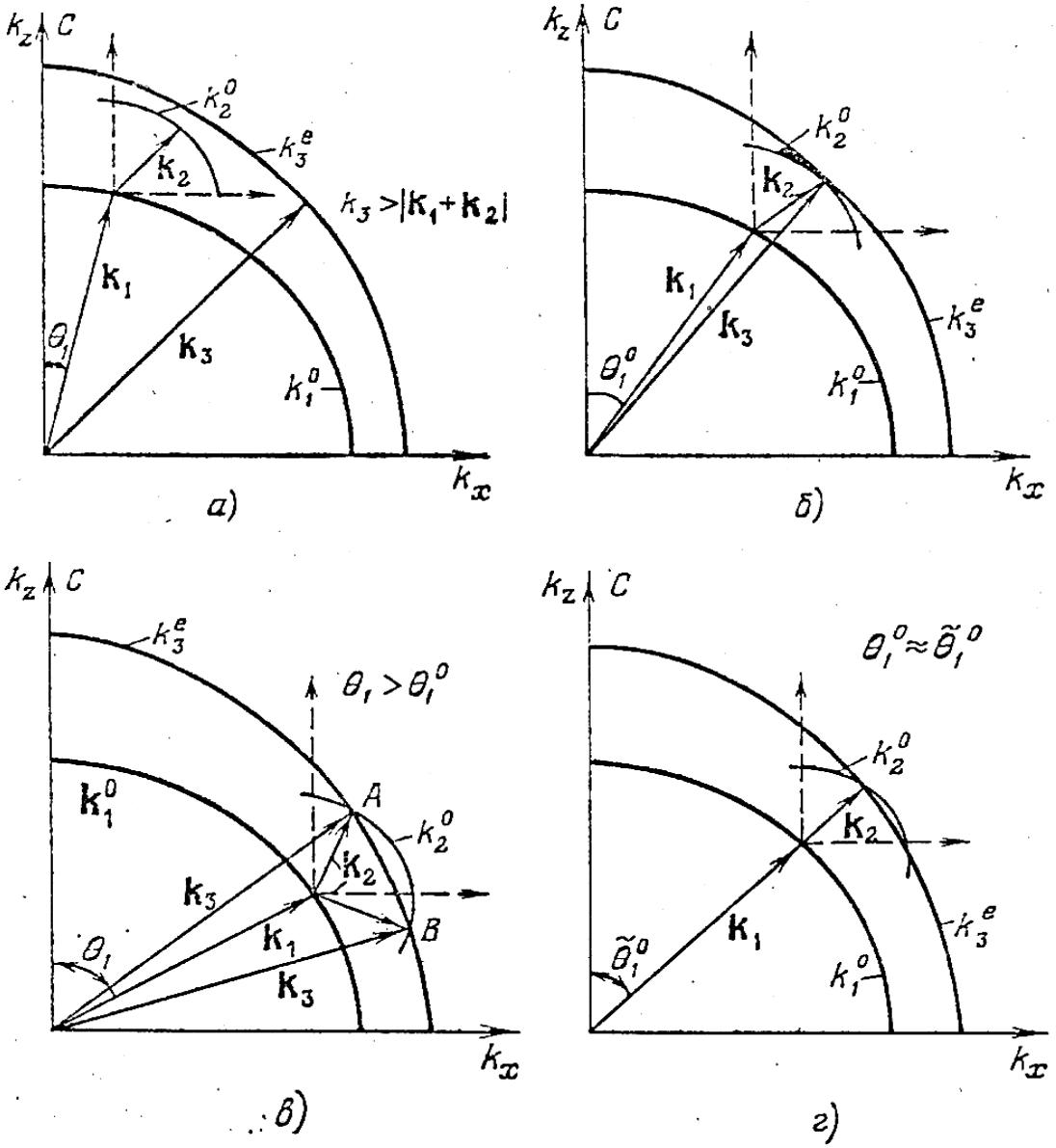

Figure 2.1 – Mutual arrangement of the wave vectors $\mathbf{k_i}$ surfaces at frequencies ω_i with ***ooe*** interaction; C is the optical axis of the crystal. *a*) There is no matching for any k_2, *b*) tangential matching, *c*) critical vector matching, *d*) one-dimensional critical matching

Let us represent the surface of the wave vector $\mathbf{k}_1$ as a sphere and fix some direction. Taking the end of this vector as the origin of a new system with axes parallel to the original system, we construct a spherical surface for the vector $\mathbf{k}_2$.

In the original coordinate system, the surface of the vector $\mathbf{k}_3$ will be an ellipsoid of revolution.

Different situations are possible depending on the angle θ_1. As long as the latter is small enough (Fig. 2.1a), $\mathbf{k}_3 > |\mathbf{k}_1 + \mathbf{k}_2|$ for any direction $\mathbf{k}_2$ due to normal dispersion in the transparency region ($n_{3o} > n_{1,2o}$). However, due to the curvature of the $\mathbf{k}_3$ surface, at a sufficiently large θ_1, the surfaces $\mathbf{k}_2$ and $\mathbf{k}_3$ can touch each other (the case of Fig. 2.1b), if the degree of anisotropy is sufficiently large. For the contact point, the triangle of vectors $\mathbf{k}_{1,2,3}$ closes, and the condition $\mathbf{k}_1 + \mathbf{k}_2 = \mathbf{k}_3$ is met. This case is called non-critical or tangent matching. With a further increase in θ_1, there is an intersection at two points A and B instead of touching (Fig. 2.1c). Such geometry of wave vectors is referred to as critical vector matching. Near the direction of tangential matching, there is a collinear (one-dimensional) critical matching shown in Fig. 2.1g. In this case, the angle between the optical axis of the nonlinear crystal and the wave vectors of the interacting waves is also referred to as the angle of phase (wave, spatial) matching.

In negative crystals, phase matching can be implemented for the interactions of the ***oee*** and ***eoe*** (type II) types. However, in this case, the wave vector surfaces of the corresponding extraordinary rays in the diagrams in Fig. 2.1 will be ellipsoids of revolution rather than spheres.

It is sum frequency generation that is used to detect infrared radiation since IR detectors are quite often expensive or imperfect. For example, in a nonlinear optical crystal, an IR signal with a ω_2 frequency can be mixed with auxiliary radiation in the visible range ω_1, which is usually called pumping, while the wave at the sum frequency ω_3 also belongs to the visible spectrum region. It can be filtered from the pump and the signa, and registered with a common photodetector operating in the visible spectral range. When imposing some restrictions, not very severe, on the quality of the pump radiation (divergence, monochromaticity), that at the sum frequency retains the information contained in the spatial-angular, spectral, and time structures of the signal. Thus, based on this effect, it is possible to create nonlinear optical IR image recorders, IR spectrometers, and IR photochronographs with the highest possible resolutions of the most precise instruments in the visible spectrum region.

2.1.5 Third harmonic generation using SFG

Today, in solid-state laser systems, the third harmonic of radiation is obtained by the sum of the residual fundamental radiation after SHG and its own second harmonic in a nonlinear optical crystal, i.e. there is the sum frequencies generation (parametric frequency up-conversion) of the form:

$$\omega + 2\omega = 3\omega$$

In real laser systems, beams coming out of a nonlinear doubler with frequencies ω and 2ω are polarized orthogonally. Therefore, for a nonlinear crystal, in which the sum of frequencies results in the third harmonic, an

interaction of the oee or eoe type is to be used. In this case, collinear matching will be implemented according to the scheme shown in Fig. 2.1d.

2.2 Questions

1. Which of the medium polarization terms is responsible for the generation of the third harmonic and sum frequencies?
2. What is the difference between the conditions of phase matching in the generation of the second harmonic and sum frequencies?
3. What is the technological challenge of generating the third harmonic in crystalline bodies?
4. What types of matching are possible with ooe interaction when obtaining the third harmonic due to the generation of sum frequencies?
5. Where is the sum frequency generation used?

2.3 Laboratory part

1. After the lecturer's instruction, turn on the laser complex and set up the equipment to generate the third harmonic in the frequency mode (10 Hz) according to the quick guide given in Chapter 5.
2. Use a filter holder to place a light filter, which reduces the energy to values in the range of 50 - 100 mJ, in the path of the laser beam, based on the specification data for the energy of the output radiation of the third harmonic. Choose the light filter using the optical glass catalog and then measure the transmission of the light filter at the desired wavelength using the SF-56 spectrophotometer, according to the instructions and/or the lecturer's advice.
3. Install the energy meter PE50BF-C + Nova after the light filter. Turn on the device and set it to measure energy at a wavelength of 355 nm, according to the instructions and/or the lecturer's advice.
4. Measure the radiation energy of the third harmonic for at least 30 laser pulses.
5. Repeat steps 1-4 to measure the output energy for the second harmonic and fundamental frequency. After completing the measurements, turn off the laser complex.
6. Enter the experimental data obtained into table 2.1.

Table 2.1 – Experimental data for laboratory work №2

λ	E_{av}	n	σ	T_f
nm	mJ	num.	mJ	%
1064				
532				
355				

E_{av} {Avg} – average value of the measured energy, according to the Nova meter;

n {POINTS} – number of energy measurements, according to the Nova meter;

σ {Std Dev} – standard deviation, according to the Nova meter;

T_f – filter transmittance coefficient at a specified wavelength, measured on an SF-56 spectrophotometer.

7. Calculate the coefficients of radiation conversion of the fundamental frequency into the second and third harmonics, and set the confidence intervals of the obtained values. The report is to contain all formulas and mathematical calculations. Present the data obtained in the form of Table 2.2.

Table 2.2 – Processing data obtained in the laboratory work

λ	E_{av}	n	σ	T_f	E_{pas}	η_{pas}	E_{exp}	t(n)	ΔE	η_{exp}	$\Delta\eta_{exp}$
nm	mJ	num.	mJ	%	mJ	%	mJ		mJ	%	%
1064											
532											
355											

E_{pas} – value of the laser radiation pulse energy, according to the specification;

η_{pas} – conversion coefficient of radiation into harmonics, based on specification;

E_{exp} – average value of the laser radiation pulse energy, taking into account the transmission of the light filter;

t(n) – Student's coefficient at a confidence level $\alpha = 0,95$;

ΔE – confidence interval of laser radiation pulse energy, calculated as a random error of multiple measurements;

η_{exp} – conversion coefficient of fundamental frequency radiation into harmonics, calculated on the basis of experimental data;

$\Delta\eta_{exp}$ – confidence interval of the conversion coefficient of fundamental frequency radiation into harmonics, calculated as an error in indirect measurements.

8. Based on the data obtained, conduct a comparative analysis of experimental results and specification, and give their interpretation.

3 LABORATORY ASSIGNMENT "PARAMETRIC LIGHT GENERATOR"

3.1 Theoretical information

Three-wave interaction considered in the two previous sections involves energy transfer from the two waves with lower frequencies to the wave of the sum frequency. The reverse process is also possible due to the generation of a difference frequency, which can also occur when there is only one pump radiation at the sum frequency. This process is called parametric transformation. Parametric amplification and generation in the radio and microwave ranges were investigated even before the advent of lasers. It was expected that this process should also take place in the optical range, and it was actually experimentally implemented in 1965. Since then, parametric amplification and generation have become very important, as they make it possible to create sources of coherent IR radiation tunable in a wide range, the operation of which is based on controlled splitting of the pump frequency.

Despite monochromaticity of the radiation being a distinctive feature of the laser, in laser systems today it is possible to smoothly tune the radiation wavelength in a fairly wide spectral range. Various methods for implementing it classify laser systems into three types. The first type includes lasers in which a purposeful change in energy, and, consequently, in the wavelength of the working transition, is a result of external influences. An example is semiconductor lasers, in which radiation wavelength changes under the action of an external electric field, as well as due to some changes in temperature or pressure. The second type includes lasers with a wide working transition line, within which the wavelength is tuned. Dye solutions, compressed gases, or ionic crystals on color centers are used as the active medium of such lasers, and a dispersive element (prism or diffraction grating) is introduced into the resonator to select the desired wavelength. The third type includes parametric light generators (PLGs). Frequency tuning in a nonlinear optical crystal is based on the parametric interaction of light waves.

The latter phenomenon is based on the decomposition of powerful radiation passing through a nonlinear crystal into two light waves. The concept and the terminology for this effect originally appeared when considering parametric excitation and amplification of electromagnetic oscillations in the radio frequency range [2].

3.1.1 Radio frequency parametric generators and amplifiers

Parametric generators of the radio range are a resonant oscillatory system in which one of the energy-intensive (reactive) parameters L or C depends on the applied voltage or the flowing current.

Let us consider the principle of parametric amplification and generation using the example of the simplest system - an oscillatory circuit consisting of constant resistance R, inductance L and capacitance C, which periodically changes in time. The own frequency ω_0 of such oscillatory system is defined as:

$$\omega_0 = \sqrt{\frac{1}{LC}}.$$

When the capacitance is modulated, energy is exchanged between the signal source and the energy-intensive parametric element. A good example of energy exchange during capacitance changes is the well-known model with mechanical expansion of the charged capacitor plates (Fig. 3.1).

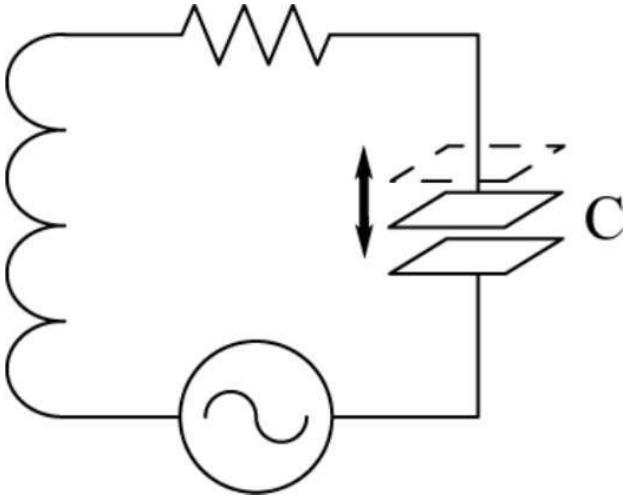

Figure 3.1 – Oscillatory circuit, in which capacitance periodically changes in time (the capacitor plates move apart)

The ponderomotive force (a non-linear force acting on a charged particle in an inhomogeneous oscillating electromagnetic field) of the capacitor electric field tends to bring the plates together (regardless of the voltage polarity). Therefore, for their expansion, i.e. for capacitance reduction, it is necessary to do some work that increases the energy reserve of the capacitor. On the contrary, when the plates approach, part of the capacitor field energy is converted into mechanical energy.

Let us consider how the electrostatic energy W stored in the capacitor changes with a change in its capacitance. When the oscillatory circuit is in resonance, the charge q on the capacitor plates changes according to the law:

$$q = q_0 \sin \omega_0 t = CQE_0 \sin \omega_0 t,$$

where E_0 is the signal amplitude, Q is the quality factor of the circuit. In this case, the electrostatic energy W stored in the capacitor will change with time with a frequency equal to twice the frequency of the signal.

$$W = \frac{q^2}{2C} = \frac{q_0^2}{4C}\left(1 - \cos 2\omega_0 t\right)$$

If at the moment when $q = q_0$, the capacitor plates are moved apart, that is, the capacitor C capacitance is changed abruptly by the value ΔC, then the charge q will have no time to change, and the energy W will change by the value (if $\Delta C/C << 1$):

$$\Delta W = -\frac{W\Delta\Delta}{C}.$$

Thus, we can conclude that for an increase of the energy in the circuit, it is necessary to periodically change the capacitance of the capacitor with a certain phase and with a frequency $\omega_p = 2\omega_0$. That is, if the capacitance is reduced at the moments when q is maximum, and the capacitance value is returned to its original value at q = 0, then the device that changes the capacitance of the capacitor C, "pumps energy" into the circuit twice during the oscillation period. In the simplest single-circuit parametric amplifier, a semiconductor parametric diode is normally used as a device that changes the oscillatory system capacitance, which depends on the harmonic voltage magnitude of the pump generator applied.

The amplification coefficient according to power can be estimated as:

$$K = \frac{1}{1 - Q\frac{m}{2}},$$

where $m = (C_{max} - C_{min})/(C_{max} + C_{min})$ is called the depth of capacitance change. The amplification coefficient increases without restrictions for $Q(m/2) \rightarrow 1$ and the system turns into a parametric generator for $Q(m/2) > 1$. The main disadvantage of a single-circuit parametric amplifier is the dependence of K on the ratio between the phases of the amplified signal and the pump signal.

This disadvantage is not present in parametric amplifiers containing two or more circuits. The schematic diagram of a two-circuit amplifier is shown in Fig. 3.2.

A two-frequency parametric amplifier consists of two circuits (signal and idle), as well as a nonlinear capacitance C_{NL} and a pump generator. The signal circuit is formed by elements L_1, C_1, G_{H1}, and the elements L_2, C_2, G_{H2} form an idle circuit. Periodic changes in the magnitude of the nonlinear capacitance C_{NL} are achieved by applying a control pump E_p voltage.

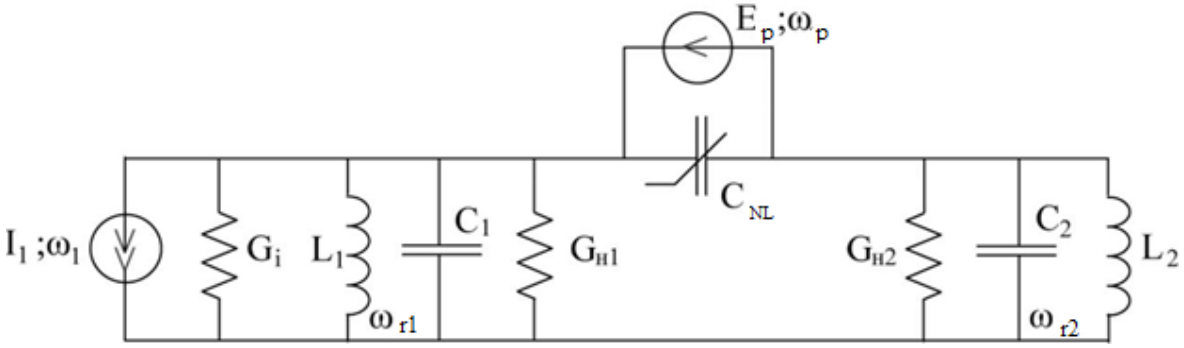

Figure 3.2 – Equivalent circuit of a two-frequency parametric amplifier

The signal circuit is tuned to the resonant frequency ω_{r1}, equal to the frequency of the amplified signal shown in Fig. 3.2 in the form of a current generator I_1. In this case, the idle circuit is tuned to the resonant frequency ω_{r2}, which is very different from ω_{r1}. It is necessary to impose some conditions on the resonant frequencies of the signal and idle circuits, under which only a signal of frequency ω_1 will exist on the signal circuit, and frequency ω_2 will exist on the auxiliary circuit. Thus, when choosing the frequency ω_{r2}, the frequency of the signal ω_1 is to be outside the passband of the auxiliary (idle) circuit. On the other hand, the combination frequency ω_2 is to be outside the operating band of the signal circuit.

Depending on how the idler is configured, this circuit can be a regenerative or non-regenerative amplifier. If the idle circuit is tuned to the frequency $\omega_2 = \omega_p - \omega_1$, then the pump energy is spent on amplifying oscillations in both circuits. Such an amplifier is called regenerative. When $\omega_2 = \omega_p + \omega_1$, all the pump energy as well as the energy accumulated in the signal circuit are converted into the oscillations energy of the total frequency $\omega_p + \omega_1$. Such a parametric amplifier is called a non-regenerative transducer amplifier.

The operation principles of parametric generators and amplifiers in the radio range described above are also used to excite oscillations in the optical range. However, there is an important difference in nonlinear phenomena in the optical range compared to the radio range. For example:

• it is intuitively obvious that the energy exchange between different frequencies occurs at the “level of currents” in the radio range, and during parametric generation, the pump source current frequency ω_p is tuned to the currents of the given frequencies ω_1 and ω_2. This naturally occurs in the corresponding two-circuit scheme by changing one of its reactive elements. However, in the optical range, there is a parametric interaction of the light waves themselves propagating in a nonlinear medium;

• in the radio range, there is no concept of "nonlinear medium", and it is semiconductor devices, vacuum tubes or other devices with non-linear characteristics that are used to observe nonlinear phenomena, while in the optical range, nonlinear optical phenomena occur directly in nonlinear media;

• in the radio range there is nothing similar to nonlinear phenomena arising in the optical range as a result of the quantum properties of radiation either.

3.1.2 Parametric light generation (PLG)

Parametric light generation in nonlinear crystals can be regarded as a process inverse to the generation of sum frequencies. It consists in converting the energy of the pump wave into two waves with lower frequencies, which in total are equal to the pump frequency. These waves are called signal and idle waves, borrowing the terminology from radiophysics.

In the corpuscular representation, the phenomenon of parametric light generation can be described as the process of a photon with ω_3 disappearing to

form two photons with frequencies ω_1 and ω_2. In this case, the total energy and the momentum are conserved, i.e. the condition of the so-called phase matching is to be met:

$$\omega_3 = \omega_1 + \omega_2$$
$$k_3 = k_1 + k_2$$

This condition cannot be met for isotropic crystals in the region of normal dispersion even in the case of vector phase-matching, when the wave vectors have different directions. However, in anisotropic crystals, the phase-matching condition can be met between the ordinary and the extraordinary waves. In a general case, matching can be achieved with four types of interaction, where the indices "o" and "e" for the wave vectors correspond to ordinary and extraordinary rays. For a BBO (β-barium borate), crystal, which will be studied in the assignment, matching can be implemented by the interaction of the ***eoe*** type:

$$k_3^e = k_1^o + k_2^e$$

There is also a distinction between scalar and vector matching. If the directions of pump radiation, signal, and idle waves are collinear, then it is a scalar (collinear) version of phase matching. In the case of the waves interacting non-collinearly, it is the concept of vector phase matching that is used.

To describe the process of parametric light generation, let us consider an intense light wave with a frequency ω_p (p refers to a pump wave) and a weak wave with a frequency ω_i (i refers to an idle wave), which propagate in a nonlinear crystal (parametric noise wave, or thermal fluctuation). As a result of the nonlinear medium polarization, a wave with a frequency ω_p forms beats with a wave having a frequency ω_i, which results in a polarization component with a frequency $\omega_s = \omega_p - \omega_i$ (s refers to a signal wave). When the phase matching condition is met , the intensity of the light wave with the frequency ω_s will increase as it passes through the crystal. In the future, beats also occur between waves with a frequency ω_s and ω_p, which results in a polarization component with a frequency $\omega_i = \omega_p - \omega_s$. This polarization will cause the wave ω_I to grow. Consequently, energy will be transferred to waves with frequencies ω_s and ω_i from a wave with the frequency ω_p.

3.1.3 Parametric luminescence and light generation

Although the physical aspects of PLG are largely similar to those in common lasers, there are some fundamental differences due to the spatial-frequency dependences of parametric luminescence. Besides, whereas in laser physics, the discovery of spontaneous (luminescence in an active medium) and stimulated (amplification of light in a medium with population inversion) radiation preceded the appearance of lasers as such, in the history of parametric light generators, the sequence was different. The PLG principles were proposed in 1962, parametric amplification and parametric generation were obtained in

1965, and parametric luminescence (spontaneous parametric light scattering) was discovered much later, in 1967.

Before the first PLG was launched, a number of researchers in the USA (Wang and Reisett) and in the USSR (S.A. Akhmanov and team) in 1965 simultaneously and independently reported the first observations of parametric light amplification in quadratically nonlinear media. Thus, Wang observed parametric amplification of the signal wave (ω_s) of helium-neon laser radiation (632.8 nm) in an ammonium dihydrogen phosphate (2nd ADP) crystal pumped by the second harmonic (347 nm) of a ruby laser (694 nm). Radiation was detected there at an idle frequency (ω_i) with a wavelength of 767.6 nm (Fig. 3.3). The gain in a non-linear element 8 cm long was 0.7 dB, i.e. 17.6% per pass. Apparently, this small amplification would definitely be insufficient to excite parametric generation (if this crystal is placed in a resonator). The experiments of S.A. Akhmanov and his colleagues recorded an amplification of about 2.5 per pass.

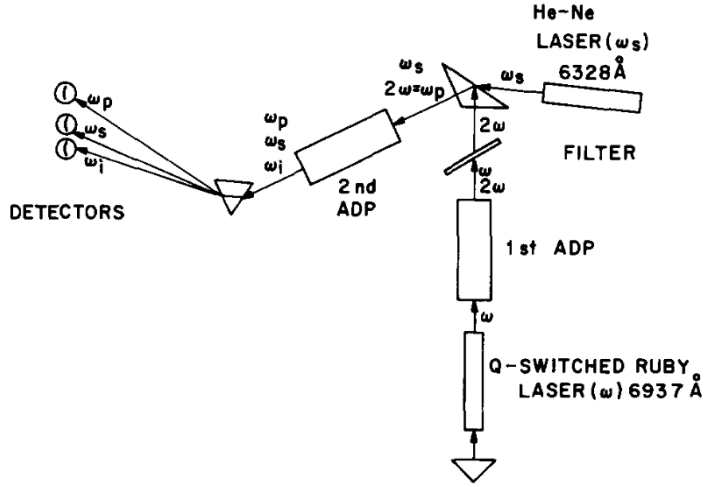

Fig. 1. Schematic of the experimental arrangement.

Figure 3.3 – Optical scheme of the experiment published in the article "Measurement of parametric gain accompanying optical difference frequency generation" in the journal "Applied Physics Letters" in 1965 (volume 6, number 8, p. 169)

In their experiment on parametric light amplification, Wang and Reisette used an intense pump light beam at a frequency ω_p, and a weak radiation beam at a frequency ω_s. However, for parametric light generation, there is no need to introduce an additional weak radiation beam with a frequency ω_s from an external source, since the radiation at a frequency ω_s is generated inside the crystal due to the so-called parametric noise or thermal fluctuations that are always present. The use of an optical resonator multipass scheme, subject to the conditions of phase matching for the desired frequencies ω_s, makes it possible to isolate and amplify the radiation of these very frequencies from this noise. These radiations will have all the characteristics inherent in laser radiation. Moreover,

if the amplification factor due to the parametric effect is large enough, then it is possible to avoid an optical resonator, and intense radiation at frequencies ω_s and ω_i, which are from parametric noise, can be obtained in one pass through the crystal. The condition for self-excitation of parametric generation in a resonator circuit is the parametric gain predominant over the passive and the radiative losses in the resonator, which is similar to the theory of conventional lasers.

An optical resonator can be used to increase the efficiency with parametric amplification. In this case, parametric generation may occur. Asis possible to obtain a tunable output radiation with a constant input radiation, the parametric oscillator, from a practical point of view, is a more useful device than a parametric amplifier.

Parametric light generation, as already mentioned, was first implemented experimentally in 1965. Let us consider the optical scheme proposed by the Americans Jormain and Miller (Fig. 3.4). This PLG was produced on a non-linear lithium niobate element ($LiNbO_3$, crystal 2). Reflecting interference coatings (dielectric coatings) were deposited on its ends, which made it possible to implement a high-Q Fabry-Perot interferometer. The radiation source was a calcium tungstate neodymium laser ($CaWO_4: Nd^{3+}$) with a wavelength $\lambda_0 = 1058$ nm. Using a nonlinear crystal ($LiNbO_3$, crystal 1), the master oscillator radiation was converted into the second harmonic ($\lambda_p = 529$ nm), which was the pump wave ω_p. The authors observed generation tuning in the range of 0.97–1.04 μm for a signal wave (ω_s) and 1.1–1.15 μm for idle one (ω_i) with a corresponding change in the temperature of lithium niobate ($LiNbO_3$, crystal 2), performing the so-called temperature tuning.

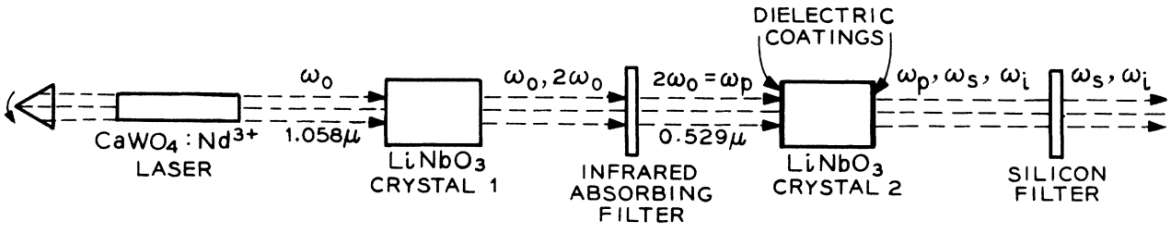

FIG. 1. Optical parametric oscillator apparatus. ω_p, ω_s, and ω_i are the pump, signal, and idler frequencies, respectively.

Figure 3.4 – The optical scheme of the PGL proposed by Jormain and Miller in the article "Tunable coherent parametric oscillation in $LiNbO_3$ at optical frequencies", published in the journal "Physical Review Letters" in 1965 (volume 14, number 24, p. 973)

3.1.4 One- and two-resonator PLG schemes

In practice, there are one- and two-resonator schemes of parametric light generation that are distinguished. A resonator of high quality at idle and signal frequencies is a two-resonator parametric light generator (TPLG). If the quality factor of the resonator is high only at one of the two frequencies, and at the other

frequency there is virtually no resonator, then it is a single-resonator parametric light generator (SPLG).

The resonator is essential because it makes it possible to select the signal ω_s and idle ω_i waves, into which the pump wave ω_p is pumped. The number of the pairs of waves, whose sum of frequencies is equal to ω_p, is infinite. However, it is the pair for which there is phase matching that will be generated, the matching direction coincides with the resonator axis, which is true for the pump wave as well.

In 1962, a scheme for a two resonator parametric light generation was proposed, using the phenomenon of parametric noise (Fig. 3.5). This scheme works using the vector matching principle, which is quite difficult to align. As shown in the Figure, the optical scheme has two resonators formed by two pairs of mirrors: one of them for the ω_s wave and the other one for the ω_i wave. Frequency is tuned by synchronously rotating the pairs of mirrors towards each other in accordance with the conditions of vector matching.

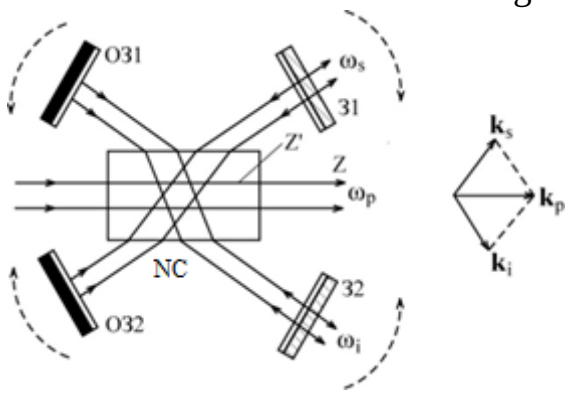

Figure 3.5 – Scheme of a two-resonator PLG: O31 is a mirror that completely reflects radiation at a frequency ω_i; O32 is a mirror that completely reflects radiation at a frequency of ω_s; NC is a non-linear crystal; 31 and 32 are the output mirrors of the resonators; Z' is the optical axis of the nonlinear crystal

A collinear version of the previous scheme is shown in Fig. 3.6a. In this scheme, a nonlinear crystal is placed between two dichroic mirrors, which operate using the phenomenon of multipath interference in thin dielectric films. The crystal is pumped by a properly focused pump beam with a frequency ω_p. Depending on the transmission of the dichroic resonator mirrors at the signal and the idle wavelengths, there are two-resonator and single-resonator PLG schemes in collinear beams (Fig. 3.6).

If the D31 mirror fully reflects the frequencies ω_i and ω_s and freely passes the frequency ω_p, and the D32 mirror also passes the frequency ω_p and partially reflects ω_i and ω_s, then this is a scheme of a two-resonator parametric light generator (Fig. 3.6a). However, if the mirrors D31 and D32 of the optical resonator are made transparent for the frequency ω_i, then the scheme will refer to a single-resonator (Fig. 3.6b)

The pump threshold is two orders of magnitude higher for a single-resonator scheme than for a two-resonator PLG. On the other hand, this results in high stability of the generated waves, in particular, the signal one.

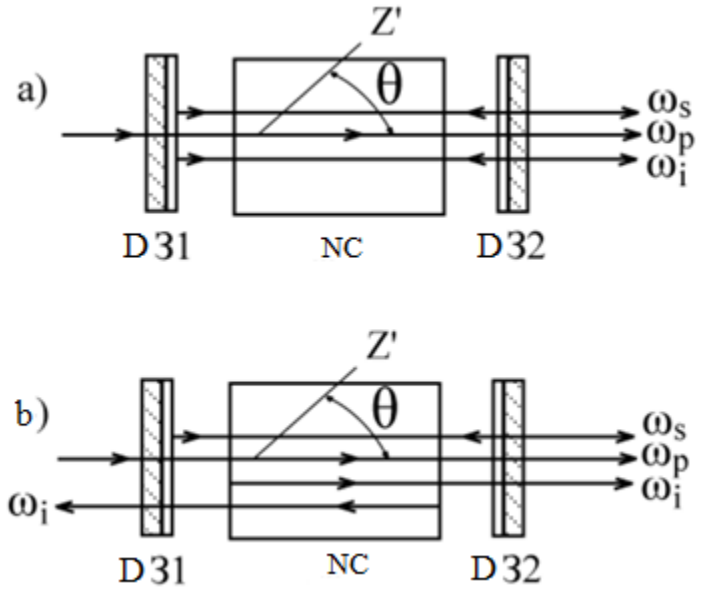

Figure 3.6 – Collinear PLG schemes: a - two-resonator scheme; b – single resonator scheme. NC is a non-linear crystal; D31 and D32 are dichroic mirrors; Z' is the optical axis of the nonlinear crystal; θ is a matching angle

The pump threshold of a two-resonator PLG can be reduced by several times by introducing a return mirror for the pump wave, which will be reflected back into the resonator. In this case, it is necessary to specifically select the phase of the reflected pump wave; otherwise, instead of parametric amplification, energy can be transferred from the parametric waves to the pump wave (regeneration of the pump wave) on the return pass. The return of the pump wave to the resonator provides parametric interaction both in the forward and reverse passes.

3.1.5 Frequency tuning with PLG

When implementing PLG devices, the main task is to create a generator scheme for tuning radiation waves in a wide spectral range. It was mentioned above that in the parametric light generation, it is those waves (those frequencies) for which the phase matching direction coincides with the resonator axis that are generated. Thus, by changing the dispersion properties (by acting on the optical axis) of the crystal, a smooth tuning of the generated radiation can be achieved.

For collinear PLG schemes, there are four methods of frequency tuning in the order of their application for the implementation in actual systems:

1) Angular tuning by rotating the crystal (its optical axis) relative to the pump beam, which corresponds to the direction of the resonator axis. This

method is the easiest to implement, and also provides a higher tuning speed, compared with those described further.

2) Temperature tuning due to heating of the crystal. Heating results in a change in the matching angle, since the refractive indices for the ordinary and the extraordinary rays depend on temperature. This method is applicable at 90° matching, i.e. when the birefringence angle is zero, and, accordingly, is used in crystals with a high dependence of the phase-matching angle on temperature: ADP (λ_p = 266 nm), $LiNbO_3$ (λ_p = 530 nm), $Ba_2NaNb_5O_{15}$ (λ_p = 530 nm), $KNbO_3$ (λ_p = 532 nm), as well as in DKDP crystals (λ_p = 266 nm).

3) Electro-optical tuning is used when an external electric field is applied to the crystal, which causes a change in the optical indicatrix. This process does not have high efficiency. Therefore, it is used only for stabilizing the generation wavelength or for high-frequency modulation of PLG radiation.

4) Tuning by changing the frequency of the pump wave ω_p. Obviously, in this case, the pump laser has to be tunable.

3.2 Questions

1. What are the similarities and differences between parametric amplification of electrical oscillations and optical parametric amplification?
2. What are the basic principles of a parametric light generator operation?
3. What is the difference between the processes of parametric luminescence, parametric amplification, and parametric generation?
4. What are the advantages and disadvantages of single-resonator and two-resonator parametric light generation systems?
5. How is frequency tuning carried out during parametric generation?

3.3 Laboratory part

1. After the lecturer's instruction, turn on the laser complex and set up the equipment for parametric light generation according to the brief guide given in Chapter 5.
2. Set the PLG wavelength indicated by the lecturer using the microscrew (position 20 in Fig. 5.8) and the data in Fig. 5.12 and 5.13.
3. Position the screen as far as possible from the PLG so that it is possible to measure the diameter of the output beam in two mutually perpendicular directions. A light filter can be used to attenuate the output radiation.
4. Move the screen as close as possible to the PLG outlet and measure again the beam diameter in two mutually perpendicular directions. After completing the measurements, turn off the laser complex.
5. Enter the obtained experimental data into Table 3.1.
6. Calculate the divergence of parametric radiation in the horizontal and vertical planes, set the confidence intervals of the obtained values. The report

should contain all formulas and mathematical calculations. Present the data obtained in the form of Table 3.2.

Table 3.1 – Experimental data for laboratory work №3

λ = _____ nm			
Micrometer screw position _____ mm			
		H	**V**
d	mm		
D	mm		
L	mm		

H and V – data for horizontal and vertical divergence;

D and d – diameters of the laser spot at different distances from the PLG outlet;

L – distance between two screen positions.

Table 3.2 – Estimated data for laboratory work №3

λ = _____ nm			
Micrometer screw position _____ mm			
		H	**V**
d	mm		
D	mm		
L	mm		
$\boldsymbol{\theta_{pas}}$	mrad		
$\boldsymbol{\theta_{exp}}$	mrad		
$\boldsymbol{\Delta\theta_{exp}}$	mrad		

θ_{pas} – radiation divergence, according to specification;

θ_{exp} – radiation divergence calculated from experimental data;

$\Delta\theta_{exp}$ – confidence interval of radiation divergence, calculated as the error of indirect measurements.

7. Based on the data obtained, conduct a comparative analysis of experimental results and specification, and give their interpretation.

4 LABORATORY ASSIGNMENT "STIMULATED RAMAN SCATTERING"

4.1 Theoretical information

The challenges associated with the wave interaction, considered in the previous chapters, definitely do not deal with electromagnetic waves only. The above analysis can be generalized by including waves of a different nature, along with electromagnetic waves, which will present many new nonlinear optical effects. Thus, stimulated Raman scattering (SRS) can be represented in the classical language as a parametric generation process, when one of the electromagnetic waves is replaced by an excitation wave of the medium. A more rigorous approach is certainly the quantum-mechanical description of the medium excitation. In this case, the SRS process is a stimulated two-photon process launched by spontaneous Raman scattering.

In a general case, light scattering is an optical phenomenon, which refers to the interaction of a medium with a light beam resulting in electromagnetic radiation of the same or a different spectral composition in the directions that differ from the original one. This definition is also suitable for photoluminescence; however, photoluminescence usually involves the absorption of an incident light quantum and the subsequent emission of another light quantum corresponding to an optical transition between the real electronic levels of the system. Scattering also takes place when a light quantum enters the region of the medium optical transparency and cannot transfer the system to a higher real level. Spectral scattering is "tied" to the exciting line, while luminescence, as already mentioned, is determined by the eigenenergy levels of the system.

4.1.1 Historical background

Light scattering without changing the wavelength, the so-called elastic or coherent scattering, was discovered in 1871 by John William Strutt (1842-1919), better known as Lord Rayleigh, and is called Rayleigh. The future Nobel prize winner believed that the gas molecular structure was enough to explain light scattering. However, later it was shown that the prerequisite is the presence of some objects in the medium that would be smaller in size than the radiation wavelength.

A little more than half a century later, it was shown that other spectral lines can be observed in the spectrum of scattered light, which are located symmetrically on the low-frequency (Stokes component) and high-frequency (anti-Stokes component) sides relative to the frequency of the incident radiation. The systems of these additional lines are different for different substances, and thus, the difference between the frequencies of the primary light wave and the additional lines characterize the natural resonances frequencies of the medium.

This phenomenon, discovered in 1928 independently by C.V. Raman and K.S. Krishnan in India and L.I. Mandelstam and G.S. Landsberg in the Soviet Union, is called combinational light scattering (CLS) in Russian sources, or the Raman effect in international sources. However, several well-known physicists theoretically had predicted the possibility of Raman scattering even before its experimental discovery. Raman scattering was first predicted by A. Smekal in 1923, followed by the theoretical exposition by Kramers, Heisenberg, Dirac, Schrödinger, and some other researchers.

In 1926, Mandelstam and Landsberg, launched an experimental study of the molecular light scattering in crystals and, in particular, sought to discover the splitting of the Rayleigh scattering line, predicted by Mandelstam in 1918, due to scattering by thermal acoustic waves. This phenomenon was later called the Mandelstam-Brillouin effect. In the related research, Mandelstam and Landsberg obtained some positive results, when, on February 21, 1928, they surprisingly discovered Raman light scattering in quartz - the appearance of satellites in the spectrum of scattered light with a frequency change that is three orders of magnitude higher than expected for the Mandelstam-Brillouin effect. The fact is that the researchers were looking for the modulation of scattered light by the acoustic frequency branch, but in fact, they registered the modulation of scattered light by the optical frequency branch. They announced their discovery at a colloquium at Moscow State University on April 27, 1928, after which, in early May 1928, they sent short reports to Soviet and German journals.

The study of light scattering in liquids began at the University of Calcutta in 1921. Raman and his student Krishnan, based essentially on the analogy with the Compton effect, assumed that some component of a lower frequency would also appear when the light was scattered. To test their hypothesis, they observed, using light filters, the scattering of sunlight in several liquids and vapors. The spectrum lines of the new radiation were first recorded by the Indians on February 28, 1928. And a week later, a brief report was sent to the journal Nature.

In general, physicists did not immediately realize that the Raman light scattering discovered by Landsberg and Mandelstam in crystals is the same phenomenon as the effect discovered by Raman in liquids and vapors. However, it was Raman who received the Nobel Prize in 1930 "for his work on the light scattering and for the discovery of the effect named after him." It has to be noted that Raman's work on his nomination for this prize was essential in this situation, while Soviet scientists did not consolidate their efforts to promote Landsberg and Mandelstam.

4.1.2 Classical Raman scattering description

Spontaneous Raman scattering of light is observed in various media - gases, liquids, and crystals. The reason for the change in the scattering frequency is a combined process, where the action of an incident light quantum produces

another light quantum and, at the same time, a certain portion of energy is absorbed or released in the medium. Generally speaking, this can result from various processes:

– periodic vibration motion of atoms in a molecule or crystal lattice around the equilibrium position,

– transitions of electrons from one level to another,

– spin waves in magnetically ordered media,

– plasma oscillations in solids, etc.

However, when describing Raman scattering, it is usually only the first process that is considered; everything is most easily described on media of diatomic molecules.

Thus, an electromagnetic wave with frequency ω and electric intensity vector $\mathbf{E} = \mathbf{E_0}\cdot\cos(\omega t)$ induces a dipole moment in the molecule $\mathbf{p} = \alpha\cdot\mathbf{E} = \alpha\cdot\mathbf{E_0}\cdot\cos(\omega t)$, where α is the polarizability tensor of the molecule. The polarization of a molecule (and of the entire medium) periodically changes in time with the frequencies of natural molecule oscillations, since the polarization at a certain moment of time depends on the arrangement of atoms relative to each other corresponding to this moment: $\alpha = \alpha(q_i)$, where q_i is the vibrational coordinate of the nuclei displacement, which varies according to the harmonic law $q_i = q_{i0}\cdot\cos(\omega_i t)$. For small oscillations, α depends linearly on q_i, therefore, by expanding α in a Taylor series in terms of the nuclei displacement coordinates q_i near the equilibrium position ($q_i = 0$), we obtain:

$$\alpha(q_i) = \alpha(0) + \left(\frac{\partial\alpha}{\partial q_i}\right)_0 \cdot q_i + \cdots \qquad (4.1)$$

Thus, the polarization of the medium is a function of the molecule atoms coordinates, which periodically change with the natural oscillations frequencies of the system:

$$p(t) = \left[\alpha(0) + \left(\frac{\partial\alpha}{\partial q_i}\right)_0 \cdot q_{i0} \cdot cos\,(\omega_i t)\right] E_0 cos\,(\omega t) = \alpha(0)\cdot E_0 cos\,(\omega t) + 0.5\cdot\left(\frac{\partial\alpha}{\partial q_i}\right)_0 \cdot E_0 \cdot q_{i0} \cdot cos\,([\omega_i - \omega]\cdot t) + 0.5\cdot\left(\frac{\partial\alpha}{\partial q_i}\right)_0 \cdot E_0 \cdot q_{i0} \cdot cos\,([\omega_i + \omega]\cdot t) \qquad (4.2)$$

This induced dipole moment should be considered as a source of secondary electromagnetic radiation that forms the scattering spectrum. The first term refers to the change in polarization with frequency ω (Rayleigh scattering), the second and the third ones correspond to the Raman spectra of the first order. If we consider other terms in the expansion (4.1), we could obtain the second and the higher orders of Raman scattering; however, the intensity of such lines is very low, and only the first Raman scattering order will be considered below. Unlike Rayleigh, Raman light scattering is incoherent,since the oscillation phases of different molecules are independent.

4.1.3 Raman scattering in terms of quantum mechanics

Figure 4.1 shows the processes of absorption and fluorescence in the visible and IR regions, as well as Rayleigh and Raman scattering with the appearance of Stokes and anti-Stokes lines. Raman scattering is shown to be an additional method to IR spectroscopy for studying the vibrational sublevels of quantum systems.

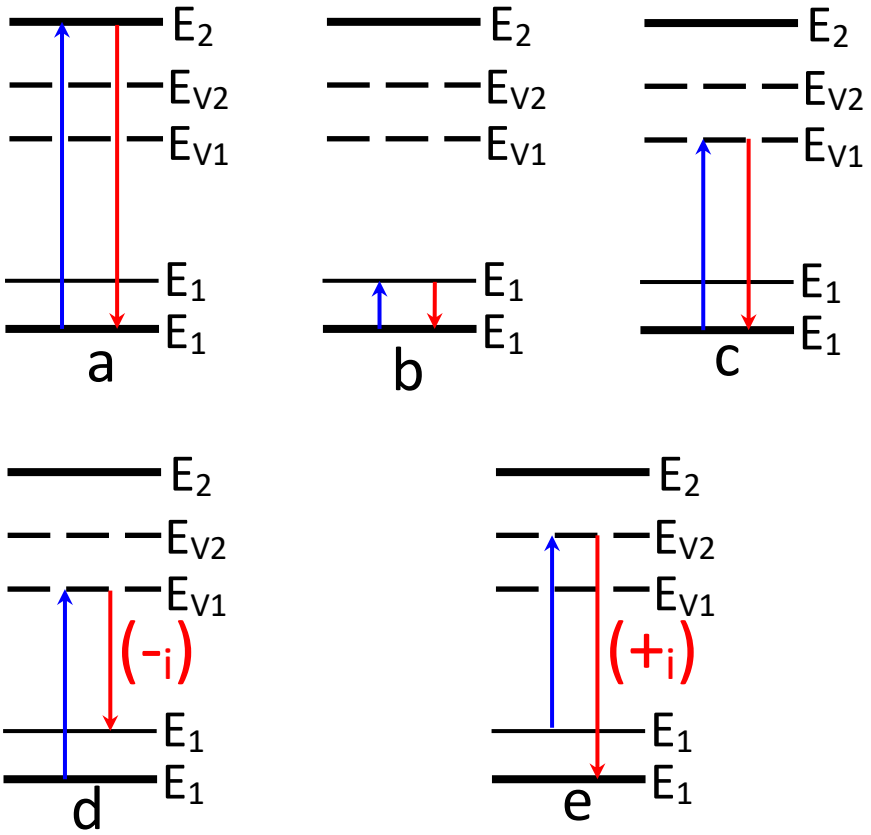

Figure 4.1 – Scheme of processes during the interaction of radiation with matter: (a) and (b) - absorption and fluorescence in the visible and IR regions; (c) Rayleigh scattering; (d) Stokes Raman scattering, (e) anti-Stokes Raman scattering

Let us consider the case of nonresonant scattering when the frequency of the exciting light ω falls into the region of medium transparency. According to quantum mechanics, the energy levels of a molecule form a discrete series E_1, E_2, … We have to introduce virtual levels E_{V1} and E_{V2}, which reflect the intermediate states of the system and are necessary to describe the interaction of light with matter. Their energy position is determined by the energy of the incident wave, which excites the scattering. At the same time, E_{1v} are vibrational sublevels of the ground state E_1, and E_2 is an excited state.

It is noteworthy that classical theory does not explain all the regularities of Raman light scattering. For example, it cannot explain the ratio between the intensities of the corresponding Stokes and anti-Stokes satellites. According to classical theory, these intensities should be almost the same. Experience shows

that the intensity of the Stokes bands is always greater than that of the corresponding anti-Stokes bands.

Quantum theory provides an obvious explanation for this regularity. The scattering of a photon by a molecule is similar to the process of its collision with a molecule, which follows the law of energy conservation. In such a process, a photon can either transfer part of its energy to a molecule, or, conversely, receive some energy from an excited molecule. According to the ratio $E_{phot} = \hbar\omega$, the change in photon energy reflects a change in its frequency. Let a photon with energy $\hbar\omega$ be scattered by a molecule with energy E_1. A scattered photon with energy $\hbar\omega_i$ appears, and the molecule passes to the energy level E_{1v}. According to the law of energy conservation $\hbar\omega + E_1 = \hbar\omega_i + E_{1v}$, so

$$\omega_i = \omega + \Omega,$$

where

$$\Omega = \frac{(E_1 - E_{1v})}{\hbar}.$$

If $E_1 > E_{1v}$, then the frequency of the scattered photon is greater than the incident one, i.e. an anti-Stokes satellite appears in scattered light. If $E_1 < E_{1v}$, then a Stokes satellite appears during scattering.

Let $E_1 < E_{1v}$. Then the red satellite will appear when the initial level is the level E_1, and the purple one appears when the initial level is E_{1v}.

For the intensity ratio of the satellites, $\frac{I_r}{I_p} = \frac{N_1}{N_{1v}}$, where N_1 is the number of molecules at the E_1, and N_{1v} is at the E_{1v}. According to the Boltzmann formula, at thermal equilibrium

$$\frac{N_1}{N_{1v}} = exp\ exp\left(-\frac{E_1 - E_{1v}}{kT}\right) = exp\ exp\ \frac{\hbar|\Omega|}{kT},$$

and therefore

$$\frac{I_r}{I_p} = exp\ exp\ \frac{\hbar|\Omega|}{kT}.$$

This formula fully explains the observed intensity ratio.

4.1.4 Selection rules for vibration types

Formula (4.2) shows that the contribution of the q_i vibration to the magnitude of the polarizability modulation depends on the value of the derivative $(\partial a/\partial q_i)_0$ at the equilibrium position of the molecule, which ultimately determines the intensity of the Raman components pair with frequencies $\omega + \omega_i$ and $\omega - \omega_i$. Vibrations to which the relative motions of atoms correspond, and which do not change the polarizability of the system, are inactive in the Raman scattering. Thus, the criterion for the activity of vibration q_i in the Raman spectra is the condition $(\partial a/\partial q_i)_0 \neq 0$. group-theoretic analysis shows that for molecules and crystals whose symmetry group includes the inversion center, there is a rule according to which the same types of vibrations cannot simultaneously be active

both in Raman scattering and in IR light absorption. Here, the light absorption is understood as the absorption of a light quantum and the birth of a vibrational quantum with the same energy. If a vibration changes the polarizability of a molecule, then it is active in Raman scattering. If a vibration changes the dipole moment of the system, i.e. can be excited by an electromagnetic wave, then it is active in IR absorption.

4.1.5 Raman scattering spectra

Vibrations of molecules can refer to changing the lengths of bonds (stretching vibrations) or the angles between bonds (deformation vibrations).

Figure 4.2 shows the Raman scattering spectrum (Raman spectrum) of liquid water (H_2O molecules in the liquid aggregate state), obtained by excitation with argon laser radiation at λ = 488 nm. The most intense line in the spectrum at 3415 cm^{-1} appears as a result of the energy exchange of the incident light with the energy of valence vibrational motions corresponding to the stretching of the O–H bond. Vibrations occurring during bending (deformation of the angle) H–O–H in a water molecule appear much weaker in the spectrum (maximum 1619 cm^{-1}).

An important feature of the water Raman scattering is that the intensity of this spectrum is low except for the stretching vibration line. This allows getting clear lines of substances dissolved in the water against its background. In this respect, Raman spectroscopy fundamentally differs from IR spectroscopy, since water very strongly absorbs infrared radiation. Besides, the technique for obtaining Raman spectra makes it possible to use any wavelength of the exciting radiation, resulting in exceeding the energy gap between the vibrational sublevels. The spectrum will not change due to the excitation wavelength changing. This is explained by the fact that there is a non-resonant interaction of light with the medium, when there is no need for the quantum energy to correspond to the energy transition in the quantum system. By changing the wavelength we can also exclude from consideration the effects resulting from the appearance of luminescence bands in multicomponent media.

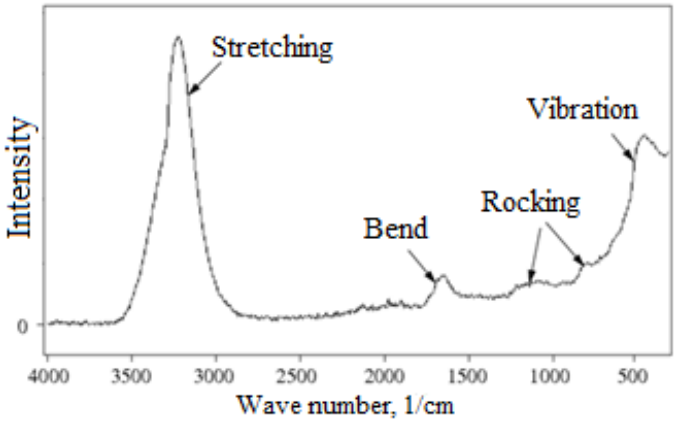

Figure 4.2 – Raman scattering spectrum of liquid water, obtained by excitation with an argon laser (λ = 488 nm)

The main comments on the intensity of lines in the Raman spectra of various substances:

– Stretching vibrations are more pronounced than bending vibrations, as can be seen from the example of water.

– Vibration lines of multiple bonds would be more intense than vibration lines of single bonds.

– The lines due to in-phase vibrations of valence bonds are more intense than those from anti-phase vibrations of these bonds.

As mentioned above, one of the issues in obtaining Raman spectra is the luminescence of various impurities in the samples, which is more probable than Raman scattering. The lifetimes even of fast luminescence (fluorescence) are known to lie in the nanosecond range, unlike the picosecond range for Raman scattering. Therefore, using picosecond lasers for excitation and a high-speed registration system that is turned off after receiving Raman radiation before the arrival of luminescence quanta eliminates the background lines from the spectrum.

It is clear from the above that Raman spectra can be used to measure the natural vibration frequencies of molecules and crystals. This opens up wide opportunities for identifying substances and studying the transformations occurring in them under external influences. So, the same substance can have several modifications, for example, carbon can have the form of graphite, diamond, and amorphous phase. Chemical or spectral analyses do not distinguish between these phases, but the Raman spectra for them will differ, since it is not only the chemical composition of the substance, but its structure as well that is important for Raman scattering. Raman can be used to study the processes of crystal melting and liquid crystallization, to investigate chemical reactions in solutions, to record the appearance of thin films on the surface of solids and characterize their structure, and for other purposes. Changes in temperature, pressure, and other external factors result in a change in the lattice symmetry of some crystals (structural phase transformations). The rearrangement of the crystal lattice naturally leads to a change in its vibrational spectrum, and Raman is a subtle tool for the analysis of these transformations.

4.1.6 Stimulated Raman scattering

Under the action of high-power laser pulses, stimulated Raman scattering (SRS) can be observed. This is a nonlinear process of radiation amplification at combination frequencies caused by the back action of a light wave on the medium molecules.

Stimulated Raman scattering was first obtained in the experiments of Woodbury and Ng in 1962 by modulating the Q-factor of a ruby laser using a Kerr cell based on a cuvette filled with nitrobenzene. In their research, they noticed it in the generated laser pulse of radiation at a 767 nm wavelength, the

power of which reached 1/5 power of the ruby laser main radiation at a 694 nm wavelength. Later, Woodbury and Eckhard suggested that the appearance of the infrared component in the spectrum results from SRS in nitrobenzene. This assumption was soon confirmed by a number of researchers on a large number of liquids. Similar effects were soon discovered in gases and solids.

The first theoretical SRS description was given a year later, in 1963, by Hellourt, who considered it as a two-photon process, and performed a complete quantum mechanical calculation. He explained the appearance of the new band as Stokes stimulated Raman scattering of ruby laser radiation in nitrobenzene (1345 cm^{-1}).

However, a simple theory cannot explain many of the facts observed in experiments, for example, the origin of the anti-Stokes radiation component, whose intensity is often as high as the intensity of the Stokes component. Experimentally observed stimulated Raman gain is also worth mentioning, as it is much larger than the predicted theoretical value, as well as a very sharp SRS threshold, asymmetry in the SRS intensity forward and backward, and a noticeable spectral broadening of the Raman components. It was later established that the anomalies are not related to the SRS mechanism, but to the self-focusing of the laser beam, whereas when there was none, the theory provided absolutely adequate explanations of the experimental results..

Initially, the interest in SRS was caused by the possibility of generating intense coherent radiation at new frequencies, and also by the fact that SRS is a possible mechanism of energy loss during propagation of high-power laser radiation in a medium, for example, during its propagation in the atmosphere or in thermonuclear plasma. Later, SRS was used to generate tunable coherent IR radiation either by tuning the excitation frequency of the medium, or by tuning the frequency of the exciting laser, for example, in a dye. The spectroscopic applications of SRS have also been developed, with an emphasis on high-resolution spectroscopy.

4.1.7 Physical SRS basis

Let us consider the classical scheme for observing SRS (Fig. 4.3). The beam of laser radiation passes through the scattering substance K and is filtered out by a light filter C. It is only scattered light with a changed frequency that is observed on the screen. The screen illumination distribution is shown schematically on the right. Near the axial point, which corresponds to the direction of the exciting radiation propagation, scattered radiation is concentrated with a Stokes frequency shift $\omega - n\omega_i$, where n refers to the order of the SRS bands. Radiation with an anti-Stokes shift forms a pattern of concentric rings, whose radius increases with the order of shift frequency additions increasing. The anti-Stokes components are observed only along the path of the exciting beam, while the Stokes ones propagate both in the forward and the backward directions.

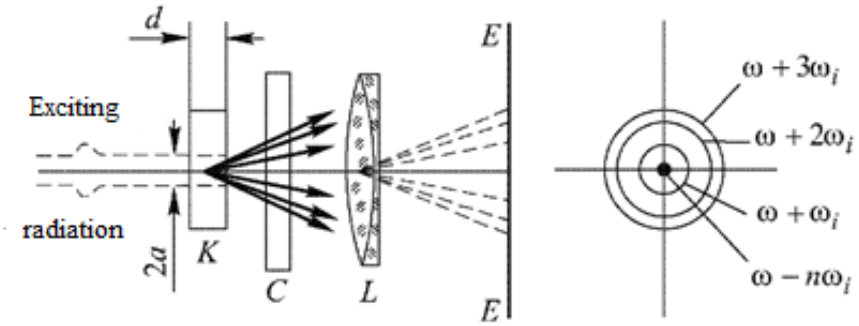

Figure 4.3 – Scheme of the experiment for observing SRS radiation: K is the edium in which scattering occurs; C is the light filter for cutting off the exciting adiation; L is the focusing system; E is screen for observing the scattered light

4.2 Questions

1. What are the types of light scattering and what is their nature?
2. How can Raman light scattering be described in terms of periodic atoms oscillations in the matter?
3. Why do Stokes and anti-Stokes Raman bands have different intensities?
4. What types of vibrations can appear in Raman spectra?
5. What are the fundamental differences between spontaneous and stimulated Raman scattering?

4.3 Laboratory part

1. After the lecturer's instruction, turn on the laser complex and set up the equipment for the generation of the third harmonic (wavelength 355 nm) according to the quick guide given in Chapter 5.
2. Assemble the optical scheme for observing SRS according to Fig. 4.3.
3. Turn on and set up the multichannel photon analyzer RMA-12 (Hamamatsu) according to the instructions for measuring the emission spectra. Place the RMA-12 detector at the point of SRS observation and measure the spectrum in the range of 300–800 nm. Turn off the laser and the device.
4. Turn on and set up the RF-5301PC (Shimadzu) spectrofluorimeter according to the instructions for measuring the emission spectra. Measure the emission spectrum in the range of 300–800 nm upon excitation at a wavelength of 355 nm, varying the spectral widths of the slits to achieve an adequate signal intensity.
5. Based on the data obtained, plot the spectra of spontaneous (measured with a spectrofluorimeter) and the stimulated (measured upon excitation by a laser source) Raman scattering (Raman shift spectra).
6. Identify the Raman bands in the obtained Raman shift spectra based on Fig. 4.2.

7. Finally, explain the nature of all the observed bands of the Raman spectrum, compare the results for stimulated and spontaneous scattering.

5 BRIEF OPERATION GUIDE FOR LQ829*LG103T*LP603 LASER COMPLEX

The laser complex [3] is designed to generate laser pulses with fixed wavelengths of 1064, 532, 355 nm and tunable wavelengths in the range from 410 to 2300 nm.

5.1 Safety precautions when working with laser radiation sources

The laser complex is a device of the 4th class of laser hazard. The output radiation is dangerous when irradiated to the eyes and to the skin by direct and reflected beams. Laser radiation can be invisible to the eye, which increases the danger to the human eye.

It is prohibited to work without grounding, with the emitter covers removed, in modes exceeding the technical data of the laser. Emergency shutdown of the laser is performed by the red "STOP" button on the remote control unit, the red "Emergency" button on the front panel of the power supply, or by turning the key to the "OFF" position on the front panel as well. Warning signs of laser danger are posted on the doors of the room in which laser installations of the highest power are located.

Do not look directly into the laser beam or its reflection. Do not look at the laser beam with the naked eye when aiming it, as observation along the axis of the laser beam greatly increases the risk of damage to the eyes as a result of reflection. The possibility of personnel approaching the intended beam trajectory must be totally excluded.

The laser should only be operated with safety goggles designed for the appropriate wavelength range. It is recommended to work in bright general lighting, so the size of the pupils is the smallest, which helps to reduce the radiation energy that can accidentally enter the eyes.

Different wavelengths have different effects on living tissues.

Ultraviolet radiation. The energy of ultraviolet radiation quanta in the wavelength range from 350 to 50 nm varies from 3.5 to 25 eV, respectively. Photons with an energy of more than 10 eV can cause the ionization of various atoms and molecules that form the basis of living tissue. The degree of damage to the skin by ultraviolet radiation depends on the absorbed radiation energy.

Infrared radiation. The low energy of infrared radiation photons (less than 1.5 eV) is insufficient to change the electronic states of the atoms that make up living tissue. The main effect of exposure is the tissue heating during the absorption of infrared radiation. As water absorbs well in the infrared range, most biological materials for these wavelengths are opaque. The penetration depth depends on the wavelength of the incident radiation. So, for example, there is a region of high transparency at wavelengths from 0.75 to 1.3 μm with a

maximum transparency in the region of 1.1 μm. At this wavelength, about 20% of the energy incident on the surface layer of the skin penetrates to a depth of 5 mm. Human skin resists infrared radiation quite well, since it is able to dissipate heat due to blood circulation, and lower the temperature of the tissue due to the evaporation of moisture from the surface. It is much more difficult to protect the eyes from infrared radiation, heat is not likely to dissipate in them, and the lens, which focuses the radiation on the retina, enhances the effect of biological exposure. All this calls for special attention to protecting the eyes from infrared radiation when working with lasers.

Visible range. On the way to the retina, the light radiation of the visible region does not experience any noticeable absorption in the tissues and substances of the eye chamber. The energy of light photons is relatively low (3.5–1.5 eV). Under normal daylight, visible light radiation causes a chain photochemical reaction in the light-sensitive substance - rhodopsin, which is part of the cells of the retina. The final result of this process is the sensation of light visual images. “Flash blindness” of a person is a phenomenon caused by the blinding effect of light, which is understood as the effect of radiation with a density level exceeding the value at which objects are clearly visible. Any light radiation is regarded as blinding when, instead of promoting vision, makes it hindered.

Upon exiting the resonator, the laser radiation collides with air molecules, carbon dioxide, the smallest dust particles, aerosols, and other particles suspended in the air. These particles scatter laser radiation, which can create energy levels that are harmful to human vision. It is reflected laser radiation that is the most dangerous. The amount of reflected energy depends on the properties of the surface of the objects located in the irradiation zone.

5.2 Technical characteristics of the laser complex

The specified parameters of the output radiation of the laser complex components shown in Fig. 5.1 are presented in Tables 5.1 and 5.2.

Table 5.1 – Parameters of laser radiation at the fundamental frequency, as well as for the second and the third harmonics, of a parametric light generator

Radiation parameters	**Measured value**
Pulse repetition rate, Hz	1 – 10
Pulse duration, ns	10
Beam diameter, mm	**8.75**
Radiation divergence, mrad	1.2
Energy stability, %	±1.2
Pulse energy at a wavelength of 1064 nm, mJ	1050
Pulse energy at a wavelength of 532 nm, mJ	420
Pulse energy at a wavelength of 355 nm, mJ	250

Parametric light generator	
<u>1st range.</u> Tuning area, nm - **signal wave** - **idle wave**	 - **410 – 530** - **1075 – 2300**
Efficiency of generation at the maximum of the tuning curve (the ratio of the total energy of pulse generation of the signal and idle waves to the energy of pump pulses from 355 nm), %	**46**
Pulse energy at the maximum of the tuning curve of the signal wave at the system output (after the Glan prism), mJ	**66**
Pulse energy at the maximum of the tuning curve of the idle wave at the system output (after the Glan prism), mJ	**21**
<u>2nd range.</u> Tuning area, nm - **signal wave** - **idle wave**	 - **540 – 710** - **710 – 1036**
Efficiency of generation at the maximum of the tuning curve (the ratio of the total energy of pulse generation of the signal and idle waves to the energy of pump pulses from 355 nm), %	**46**
Pulse energy at the maximum of the tuning curve of the signal wave at the system output (after the Glan prism), mJ	**66**
Pulse energy at the maximum of the tuning curve of the idle wave at the system output (after the Glan prism), mJ	**28**

5.3 Optical scheme of the laser complex

The optical scheme of the laser complex is shown in Fig. 5.1. The optical schemes of each of the blocks will be discussed in more detail below.

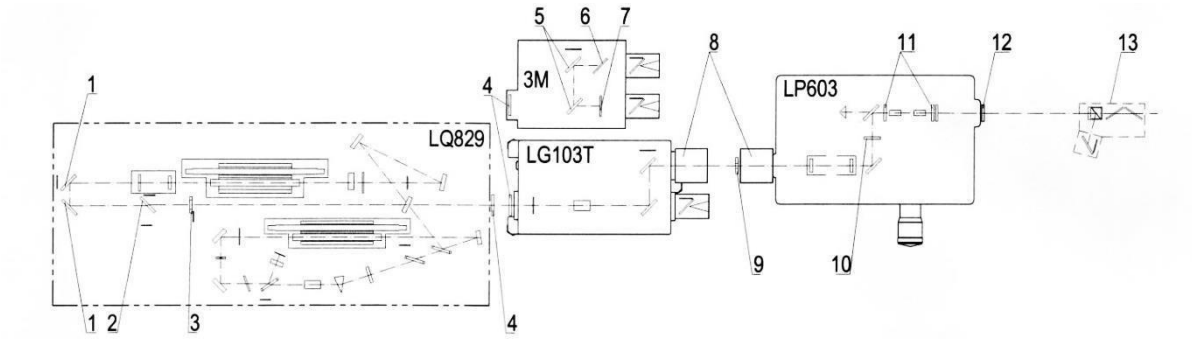

Figure 5.1 – Optical scheme of the laser complex

The pulsed Nd:YAG laser LQ829 with a built-in 2nd harmonic generator is designed to generate radiation with a wavelength of 1064 and 532 nm. Inside the laser emitter, a nonlinear KTP crystal with type II eoe phase matching is installed, where horizontally polarized radiation of the 2nd harmonic from 532 nm is generated. Also installed along the beam are:

1 – high reflective swivel mirror for 532 and 1064 nm;

2 – cutoff mirror that transmits radiation from 532 and 1064 nm and reflects radiation from 355 nm;

3 - aperture diaphragm;

4 – protective window with antireflection coatings for 532 and 1064 nm, installed in the outlet of the LQ829 laser body.

Mirror module 3M is designed for spatial separation of beams from 1064 and 532 nm. A protective window 4 is installed in the body inlet. Inside the module, along the beam path, two dichroic mirrors 5 are located at an angle of 45°, which reflect radiation from 532 nm and transmit radiation from 1064 nm. A protective window 6 with a Brewster orientation in the horizontal plane is installed in the outlet of the body for radiation at 532 nm. A protective window 7 with antireflection coatings for 532 and 1064 nm is installed in the outlet of the body for radiation from 1064 nm.

The 3rd harmonic generator LG103T is designed to generate radiation from 355 nm. Protective window 4 with antireflection coatings for 532 and 1064 nm is installed in the inlet of the LG103T case. Inside the body, along the pump beam, there is a phase plate $\lambda/4$ for 1064 nm and for 532 nm, a nonlinear DKDP crystal with type II eoe phase matching, and two dichroic mirrors, which reflect radiation from 355 nm and transmit radiation from 532 and 1064 nm. Rotating the DKDP crystal in a vertical plane provides matching adjustment. The output radiation from 355 nm is polarized in the vertical plane. A protective window 6

with a Brewster orientation in the vertical plane, in which the reflected glare is directed downwards, is installed in the body outlet.

The LP603 parametric light generator is designed to generate radiation with a tunable wavelength in the range from 410 to 710 nm (signal wave) and from 710 to 2500 nm (idle wave). An aperture diaphragm 9 is installed in front of the entrance window. A protective window 8 with a Brewster orientation in the vertical plane, in which the reflected glare is directed upwards, is installed in the inlet of the body. A telescope, a rotating mirror, an aperture diaphragm 10, a dichroic mirror-stirring, and two identical nonlinear BBO crystals with type II eoe phase matching are installed inside the body along the pump beam. Under the action of vertically polarized pump radiation from 355 nm, two waves are generated in BBO crystals: a signal with horizontal polarization and an idler with vertical polarization. The parametric generator uses two sets of nonlinear BBO crystals, one of which is designed to generate radiation in the region from 410 to 540 nm and from 1035 to 2500 nm, and the other is designed to generate radiation in the region from 520 to 710 nm and from 710 to 1116 nm. Crystals are changed manually. Inside the resonator, there are two aperture diaphragms 11. A protective window with antireflection coatings 12 is installed in the outlet opening of the body.

Polarization separator 13 is designed for spatial separation of signal and idle wave beams of the LP603 parametric generator. A Glan prism and a glass filter for cutting off radiation from 355 nm are installed inside the case. It is the horizontally polarized radiation of a signal wave in the range from 410 to 710 nm that passes in one position of the Glan prism, whereas vertically polarized radiation of an idle wave in the range from 710 to 2300 nm passes in the other position.

5.4 LQ829 block – laser and SHG

The laser contains a master oscillator and a single-pass amplifier. The operation of the laser is based on the phenomenon of light amplification due to the stimulated emission of photons by electrons in an active medium with an inverse-level population. In the laser, Nd^{3+}:YAG crystals are used as the active medium, in which, under optical pumping by a pulsed xenon lamp, an inverted level population occurs. A diffuse reflector is used to ensure efficient transmission of xenon lamp radiation to the active element.. The active element, the xenon lamp, and the diffuse reflector are located in the laser head, which has some holes for water cooling of the active element and the flash lamp.

An electro-optical shutter is located inside the master oscillator cavity. The electro-optical shutter is designed to operate the laser in the Q-switched mode. The shutter is first closed when the laser operates in the Q-switched regime, and an inverse population of the levels appears in the active medium under the action of pump radiation. This provides energy accumulation. When the population inversion in the active medium reaches its maximum value, the shutter opens

and the laser generates a short nanosecond pulse with a high peak power and a wavelength of 1064 nm. This radiation gets extra amplification in a single-pass amplifier.

A second harmonic generator is used to generate radiation with a wavelength of 532 nm. The second harmonic generation effect is based on the phenomenon of the quadratic nonlinear polarizability of a medium, in which a wave with a frequency 2ω appears with the passage of high-intensity light with a frequency ω . The second harmonic generator uses a non-linear KTP crystal with type II eoe angular matching.

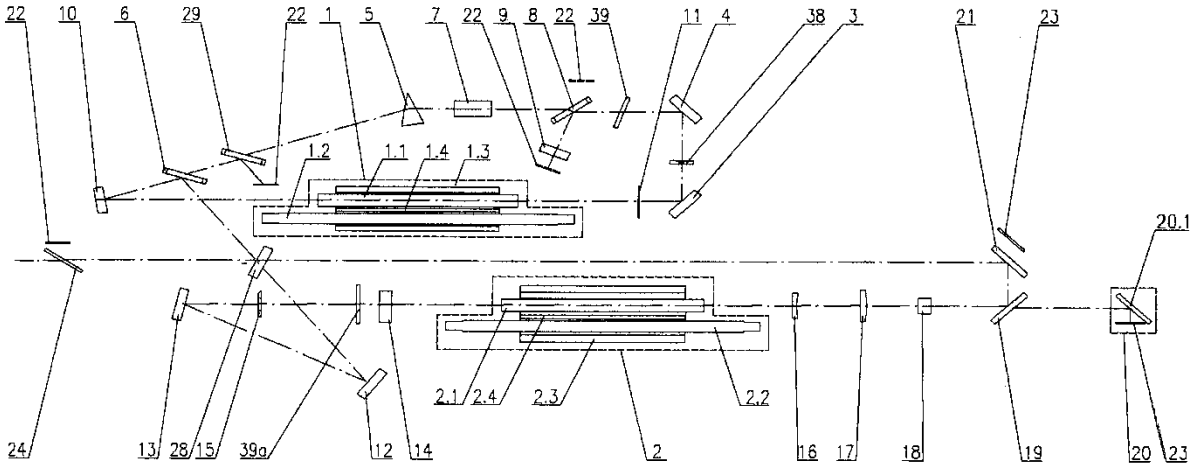

Figure 5.2 – Optical scheme of the LQ829 emitter

The optical scheme of the LQ829 emitter is shown in Fig. 5.2. Figure 5.3 shows a top view of the emitter (top cover is not shown). Identical elements in both Figures are indicated by the same numbers:

1.1, 2.1 – Nd:YAG rods of the master oscillator and amplifier;
1.2, 2.2 – pump lamps of the master oscillator and amplifier;
1.3, 2.3 – reflectors of the master oscillator and amplifier;
1.4, 2.4 – UV filters of the master oscillator and amplifier;
3, 4, 10, 12, 13 – swivel mirrors;
5 – prism;
6, 8, 29 – glass plates;
7 – Pockels cell;
9 – return mirror;
11 – phase plate;
14 – wave plate;
15, 38 – diaphragms;
16, 17 – telescope lenses;
18 – KTP crystal;
19, 21 – high reflective swivel mirror for 532 and 1064 nm;
20 – radiation trap;
22, 23 – absorbing plates;

24 – protective window;
28 – technological mirror;
39, 39a – compensators.

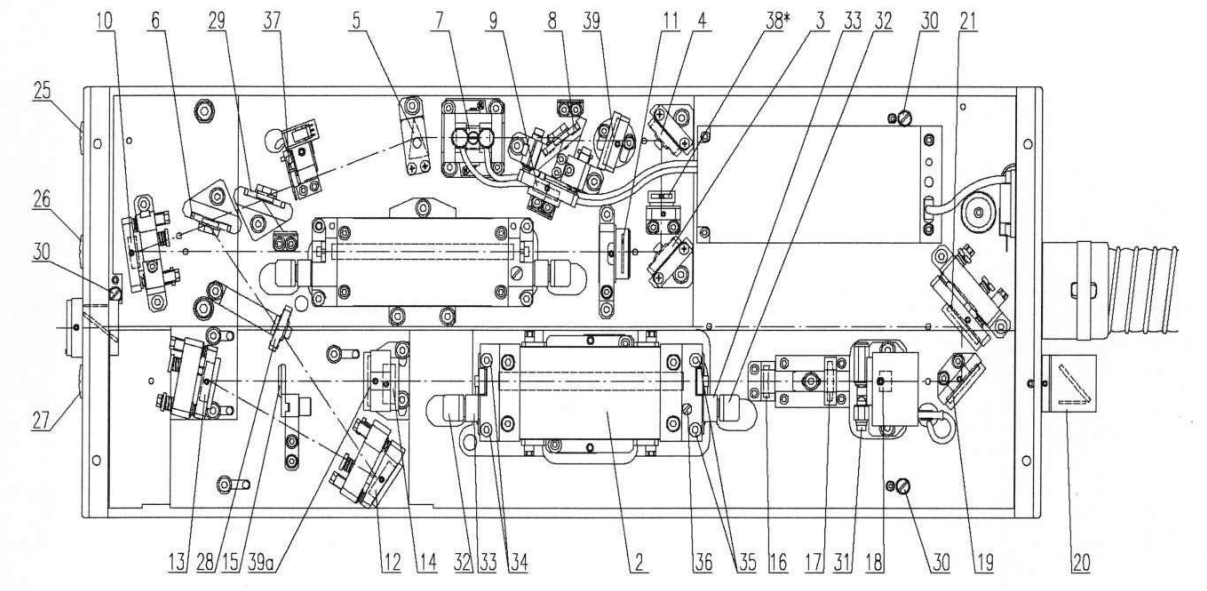

Figure 5.3 – Top view of LQ829 block

The master oscillator uses a ring resonator circuit. The resonator is formed by mirrors 3, 4, 10, and the rotary prism 5; the output mirror is plate 6 located at the Brewster angle; the return mirror 9 acts as a deaf mirror, the radiation to which is directed by a plate 8 with a dielectric coating, located at the Brewster angle. The resonator contains a laser head (1.1–1.4) and a Pockels cell 7 required for Q-switching. The lower part of the laser head contains an inlet and an outlet for the coolant. The intracavity shutter 37 serves to mechanically block the radiation, which ensures a safe pause in the laser operation.

The radiation of the fundamental harmonic (1064 nm) leaving the resonator is directed by mirrors 12 and 13 to the wave plate 14 and then to the laser head of the amplifier (2.1–2.4) and the second harmonic generator assembly containing the KTP crystal 18. Screw 31 serves to align the KTP crystal in the horizontal plane to obtain the optimal efficiency of converting the fundamental frequency to the second harmonic.

5.5 LG103 block - third harmonic generator

The LG103 generator scheme for generating the 3rd harmonic is shown in Figure 5.4, and the top view is in Figure 5.5. The same elements are marked with the same numbers:

1 – support;
2 – mounting hole;
3 – fixing screw of the input/output windows;
4 – holder of a nonlinear crystal;

5 – clamping screw of the crystal holder;

6 – screw for “rough” adjustment of the phase-matching angle of the crystal;

7 – screw for fine adjustment of the phase-matching angle of the crystal;

8 – connector for the thermal stabilization system;

9 – fixing screw of the spectrum splitter unit;

10,11 – adjusting screws of the mirror 2;

12 – node of spectrum dividers;

13 – phase plate fastening screw;

14 – screw for fastening mirror 1 and mirror 2;

15 – screw for fastening the thermostat assembly;

16 – thermostat assembly;

17 – network cable;

18 – red indicator;

19 – green indicator.

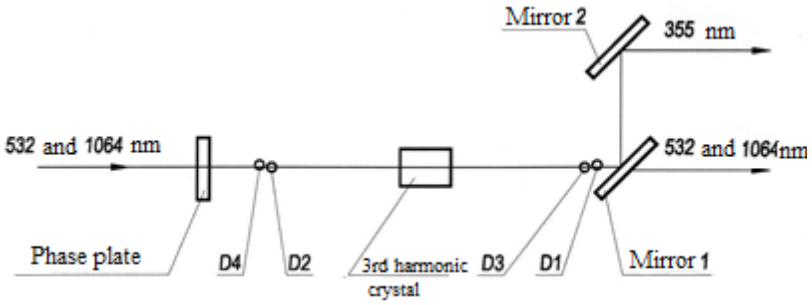

Figure 5.4 – LG103 generator scheme for generating the 3rd harmonic. Nonlinear crystal mounted in a holder without protective windows

For "rough" adjustment of the phase-matching angle in a nonlinear crystal, adjusting screw 6 is used, located near the crystal holder. To fine-tune the phase-matching angle in the nonlinear crystal, adjusting screw 7 is used, located on the side surface of the LG103 generator body.

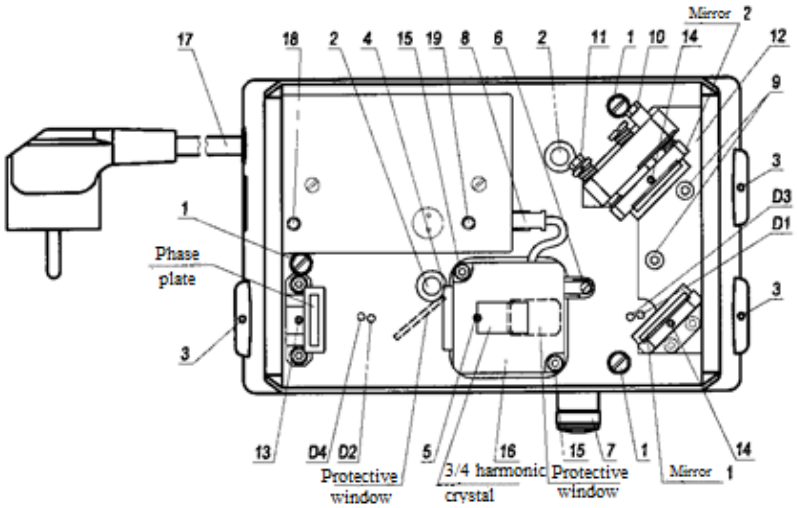

Figure 5.5 – Top view of LG103 block

The nonlinear crystal in the frame is placed in a thermally stabilized holder 4, which makes it possible to increase the stability of the output radiation. In the LG103 oscillator, a 3ω splitter assembly is used to isolate the 3rd harmonic radiation at a wavelength of 355 nm.

5.6 LP603 block – parametric light generator

PLG LP603 is designed to generate tunable radiation in the region from 410 nm to 2300 nm. The term "parametric light generation" means a phenomenon in nonlinear optics, when a pump wave with a wavelength λ_n generates two waves in a nonlinear crystal: a signal with λ_s and an idler with λ_i, for which the conditions of phase matching are satisfied:

$$\frac{1}{\lambda_n} = \frac{1}{\lambda_s} + \frac{1}{\lambda_i}$$

$$\frac{n_n}{\lambda_n} = \frac{n_s}{\lambda_s} + \frac{n_i}{\lambda_i}$$

where n_n, n_s and n_i are refractive indices of the crystal for waves with λ_n, λ_s and λ_i respectively.

At a fixed pump radiation wavelength λ_n, the wavelengths of the signal wave generation λ_s and the idle wave λ_i are tuned by changing the angle 0 between the Z axis and the pump beam propagation direction.

The LP603 PLG uses BBO crystals with type II phase matching, in which the pump and the idle waves are polarized in the vertical plane, while the signal wave is polarized in the horizontal plane (Fig. 5.6).

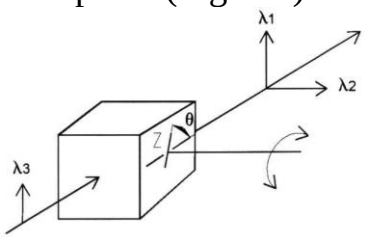

Figure 5.6 – Orientation of a BBO crystal with type II phase matching and the direction of the polarization plane of interacting waves

The optical scheme of the PLG LP603 is shown in Figure 5.7, top view is in Figure 5.8. The same elements are indicated by the same numbers in both Figures:

1 – protective window;
2 and 3 – telescope lenses;
4 and 5 – swivel mirrors;
6 – output mirror;
7-1 and 7-2 – BBO crystals;
8 – prism; 10,14,15 – screens;
11, 11.1 – diaphragms;

16 – Glan prism;

D1... D6 – the location of the adjustment diaphragms.

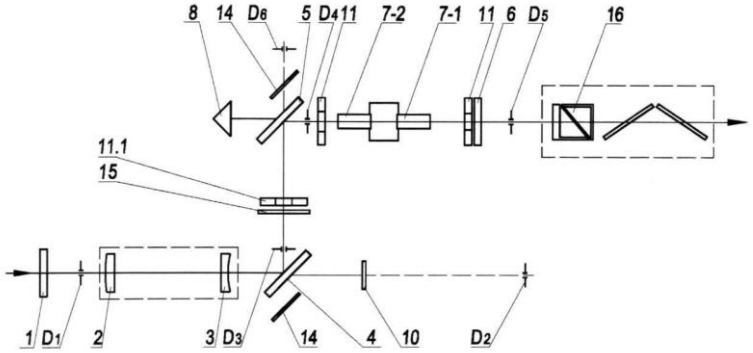

Figure 5.7 – Optical scheme of PLG LP603 with a polarization separator

The resonator is formed by the prism 8, the output mirror 6, and contains BBO crystals 7-1 and 7-2. The pump radiation passes through the telescope lenses 2 and 3 and, being reflected from mirrors 4 and 5, goes to the BBO crystals.

The PLG LP603 uses two pairs of BBO crystals with type II eoe matching. Crystals of the 1st range are marked I-1 (7-1) and I-2 (7-2). Crystals of the 2nd range are marked II-1 (7-1) and II-2 (7-2). The first pair of BBO I crystals is used to generate radiation in the 1st range of 410 – 530 nm (signal wave) and of 1075 – 2300 nm (idle wave). The second pair of BBO II crystals is used to generate radiation in the 2nd range 540 – 710 nm (signal wave) and 710 – 1036 nm (idle wave).

The generation wavelength is restructured by rotating the BBO crystals in a vertical plane. A microscrew is used to rotate the crystals, (position 20 in Fig. 5.8). To separate the signal and theidle waves at the PLG output, the Glan prism 16 is used. In one position, the Glan prism transmits horizontally polarized radiation of the signal wave 410–710 nm. In another position, the Glan prism transmits vertically polarized radiation of the idle wave 710–2300 nm.

The pump power density at the input end of the BBO crystal is to be in the range of 65 – 80 MW/cm^2. The power density of the pump pulses for the PLG LP603 is calculated by the formula:

$$P = \frac{4000 \cdot E \cdot X^2}{3.14 \cdot d^2 \cdot \tau}$$

where P is the pump power density, MW/cm^2; E is energy of pump pulses, J; X is the telescope magnification (1.3 according to the specification); τ is the pulse duration, ns; d is the diameter of the pump beam at the entrance to the PLG LP603, cm (8.75 according to the specifications).

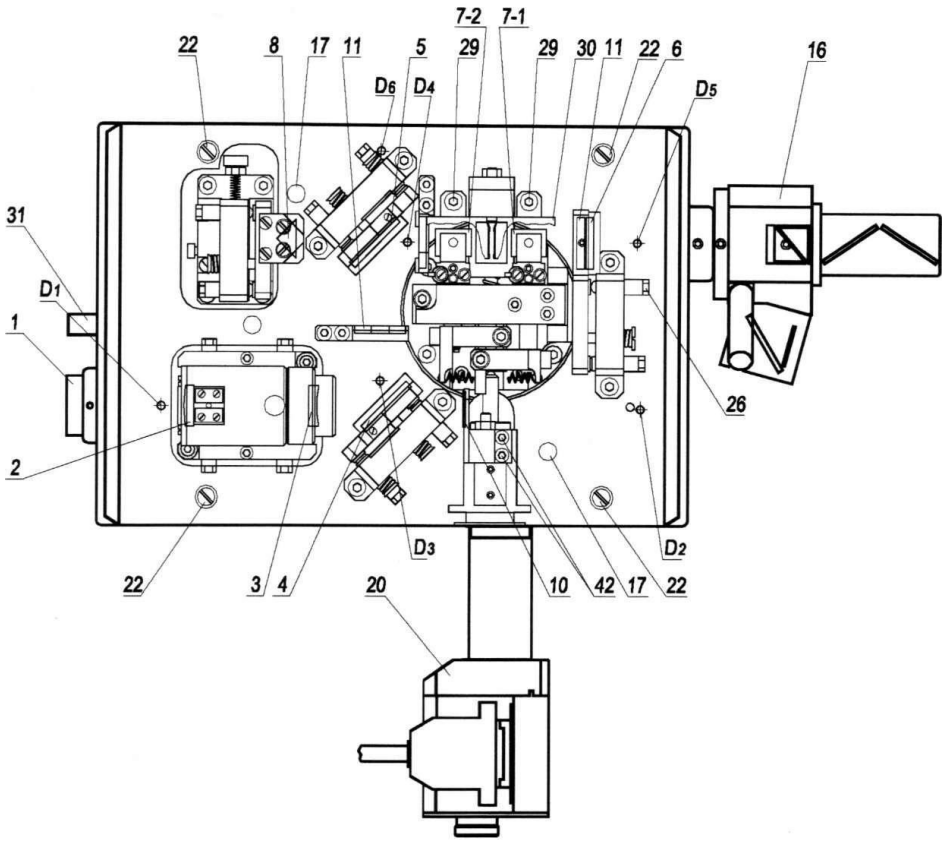

Figure 5.8 – Top view of LP603 block

In the wavelength tuning range of PLG generation, there are strong absorption bands of water vapor in the atmosphere of 1.35–1.45 μm, 1.8–1.95 μm. For long-term operation in the specified ranges, it is recommended to purge the internal cavity of the PLG with nitrogen to displace water vapor.

5.7 Operation of the laser complex

The laser complex is turned on by turning the key to the “ON” position, after which the system performs a self-test, ignites the pump lamps, and stabilizes the cooling system. When the final stabilization stage is completed, the "READY" indicator on the remote control is switched on for continuous indication.

There is a mirror module 3M and a 3rd harmonic generator LG103T on the two-position movable platform P1. A parametric light generator LP603 is located on the two-position mobile platform P2. A polarizing separator (Glan prism) is located on the two-position mobile platform PZ.

The relative position of the platforms determines the required radiation wavelength outside the laser complex. Movable platforms are equipped with interlocks: when switching the position of the platform, sensors are triggered and the laser operation stops; to resume laser operation, the positions of the platforms

are to be fixed, and have the “RESET/CLEAR” button on the remote control pressed.

5.7.1 Working with radiation with a wavelength of 1064 and 532 nm

To obtain radiation at the output of the laser system with 532 and 1064 nm, the following steps are required:

– turn the levers of the movable platforms P1, P2 and PZ clockwise and set the devices to the position shown in Figure 5.9;

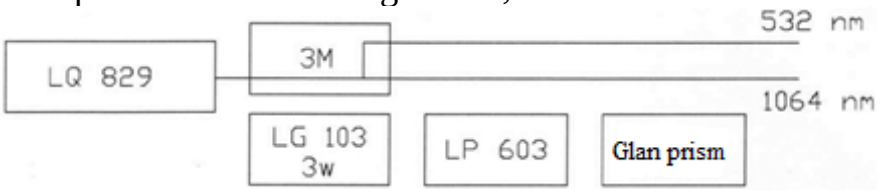

Figure 5.9 – Location of devices for generation and output of 1064 and 532 nm radiation

– turn the levers of the movable platforms P1, P2, and PZ counterclockwise and fix the position of the platforms;

– install the laser radiation plug into the required channel of the 3M mirror module;

– press successively the “OPERATION” and “Q-Switch” buttons on the remote control, after which the LQ829 laser will operate in the Q-switched mode.

5.7.2 Working with radiation with a wavelength of 355 nm

To obtain radiation at the output of a laser system with 355 nm, the following steps are required:

– turn the levers of the movable platforms P1, P2 and PZ clockwise and set the instruments to the position shown in Figure 5.10;

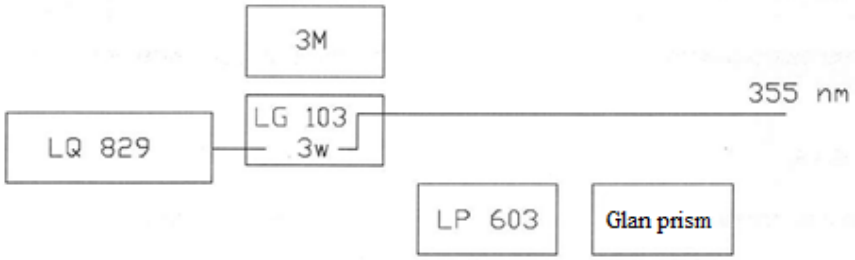

Figure 5.10 – Location of devices for generation and output of 355 nm radiation

– turn the levers of the movable platforms P1, P2 and PZ counterclockwise and fix the position of the platforms;

– press successively the “OPERATION” and “Q-Switch” buttons on the remote control, after which the LQ829 laser will operate in Q-switched mode.

5.7.3 Working with tunable wavelength radiation

A proper pair of nonlinear BBO crystals is used to obtain radiation with a tunable wavelength in the selected range at the output of the laser system. To obtain radiation with a tunable wavelength at the output of a laser system, the following steps are required:

- turn the levers of the movable platforms P1, P2 and PZ clockwise and set the devices to the position shown in Figure 5.11;

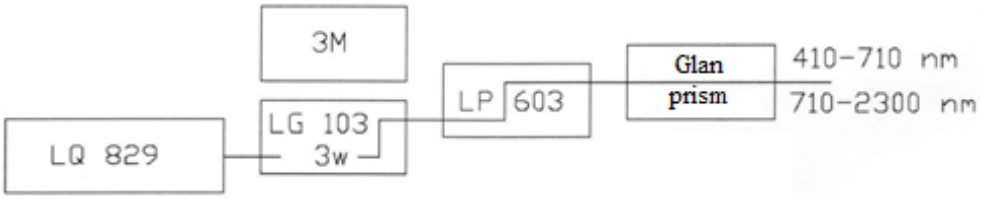

Figure 5.11 – Location of devices for working with laser radiation with a tunable wavelength

– turn the levers of the movable platforms P1, P2 and PZ counterclockwise and fix the position of the platforms.

- in accordance with the instruction manual for the PLG LP603, install the required set of crystals.

The required wavelength is set based on the tuning curve shown below in Figures 5.12 and 5.13 for different sets of crystals. The energy output data for the signal wave for the two sets of crystals is shown in Graphs 5.14 and 5.15.

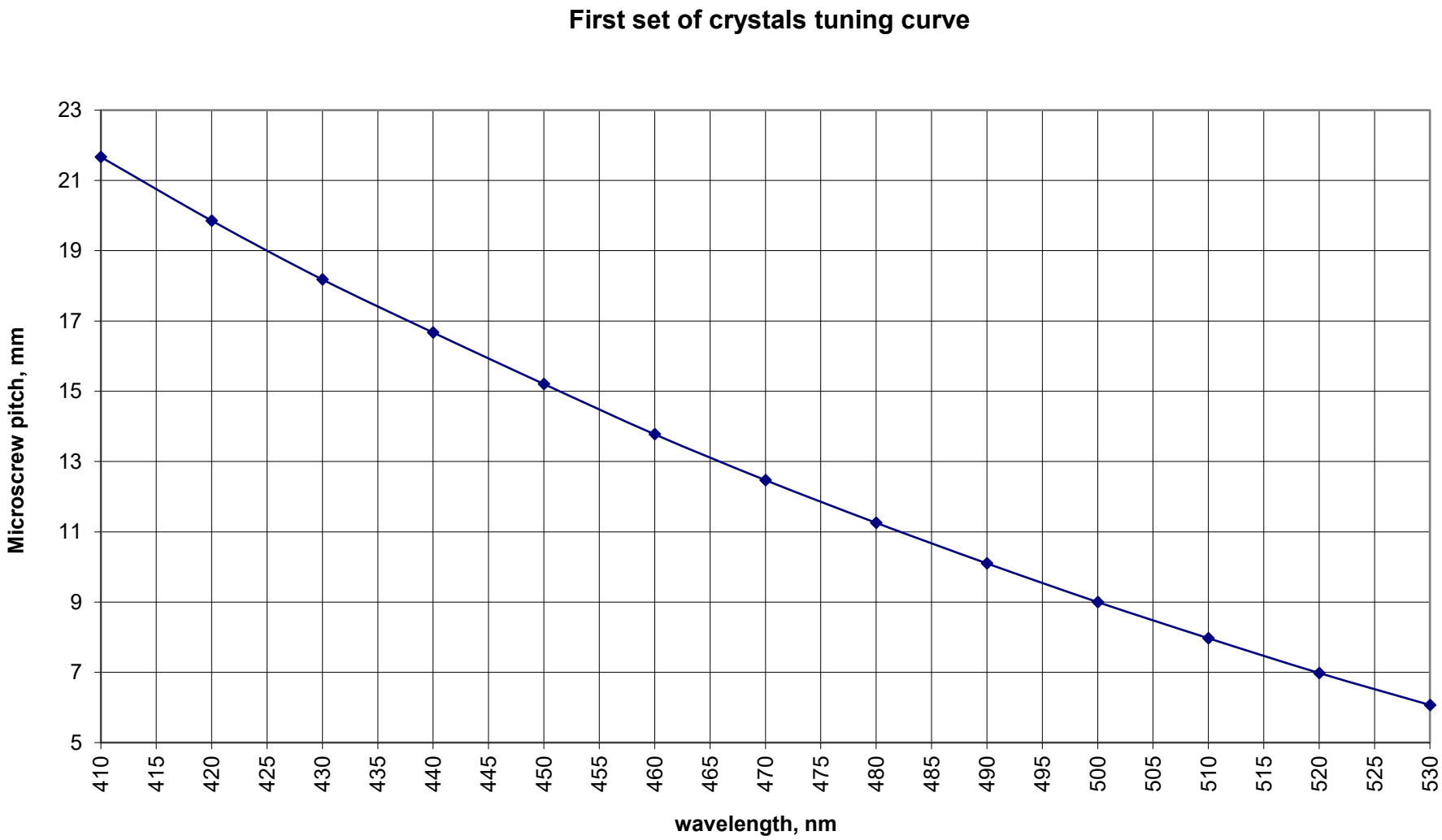

Figure 5.12 – Tuning curve for I set of crystals

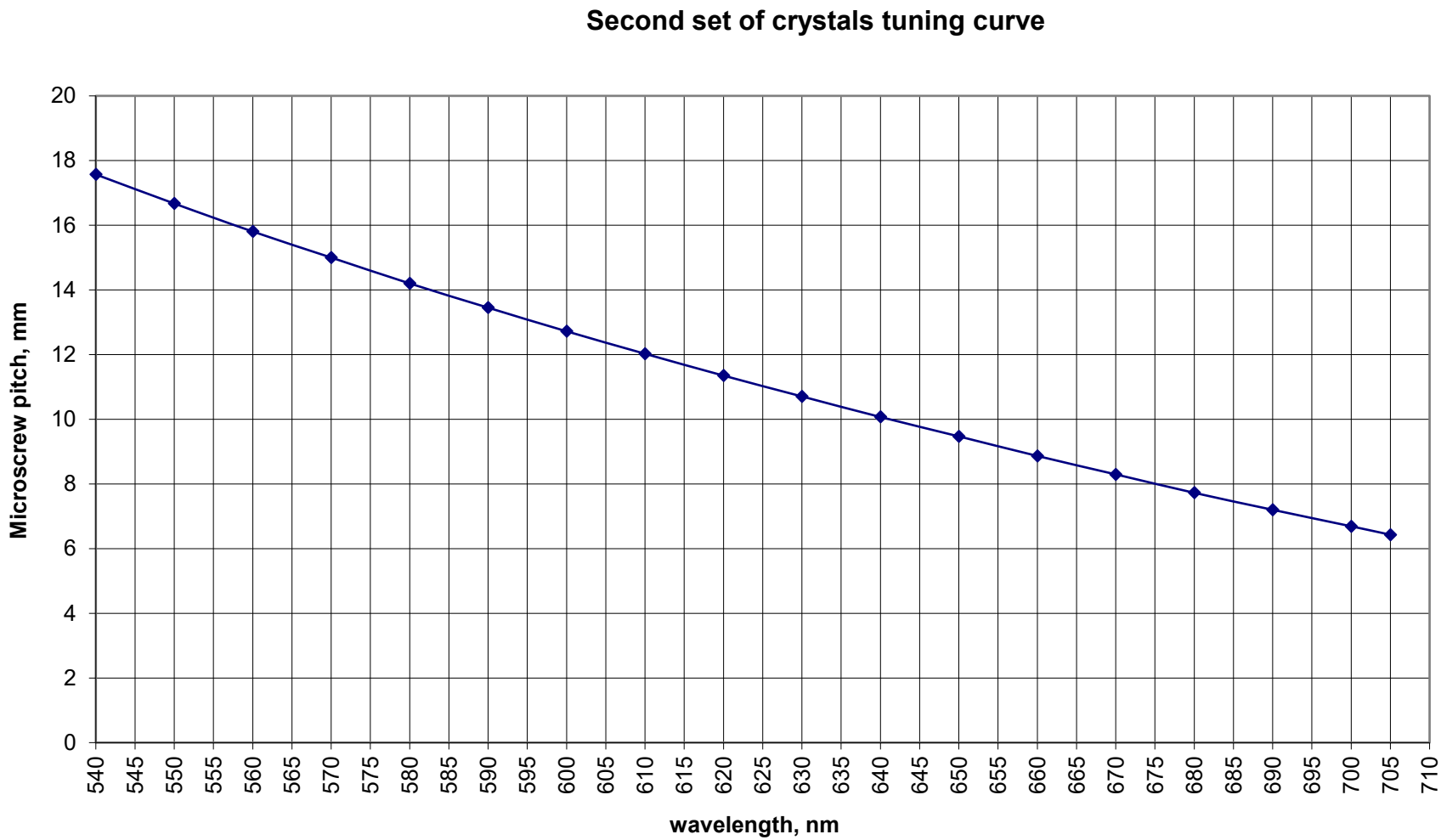

Figure 5.13 – Tuning curve for II set of crystals

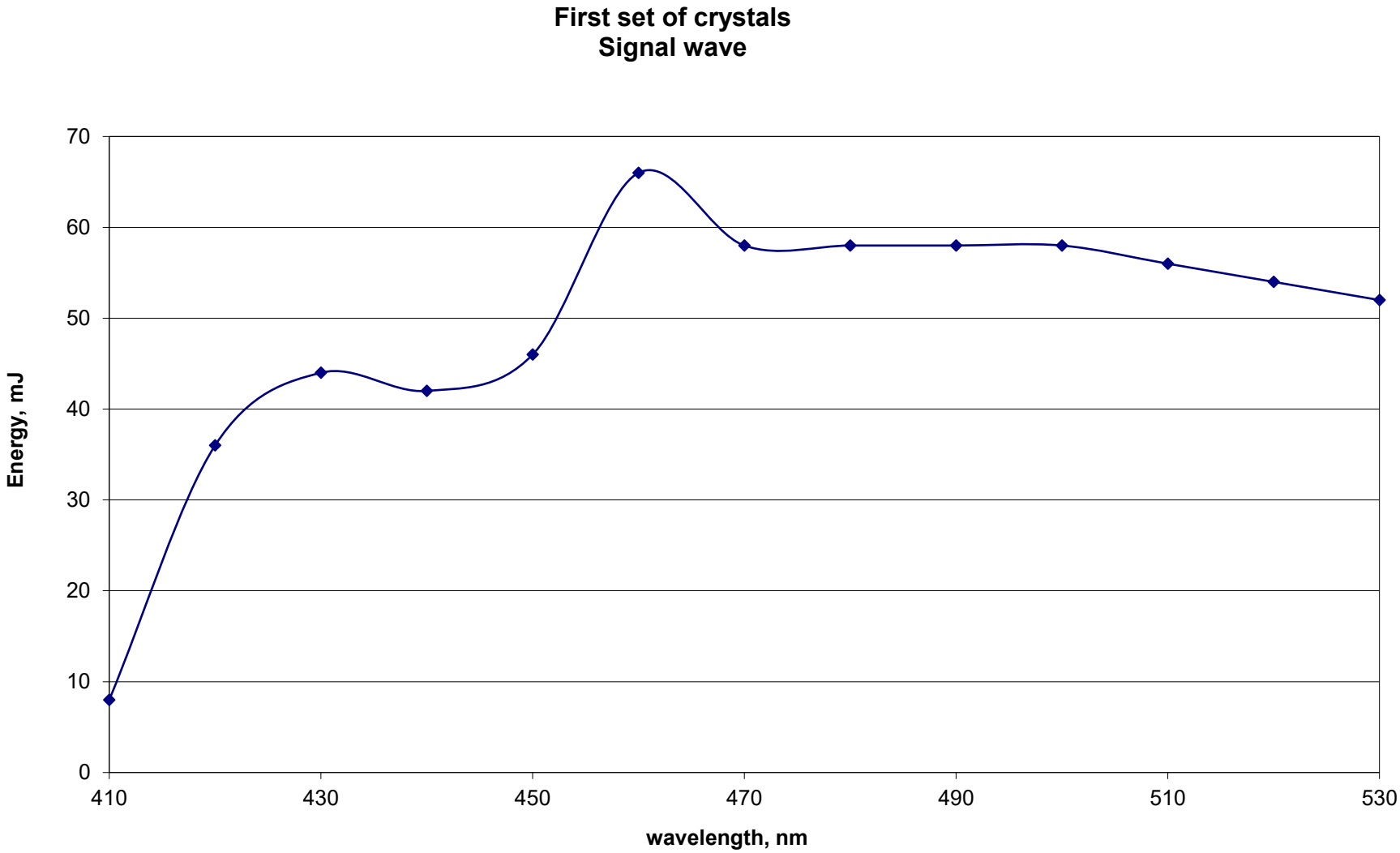

Figure 5.14 – Graph of the signal wave output energy against the wavelength for the I set of crystals

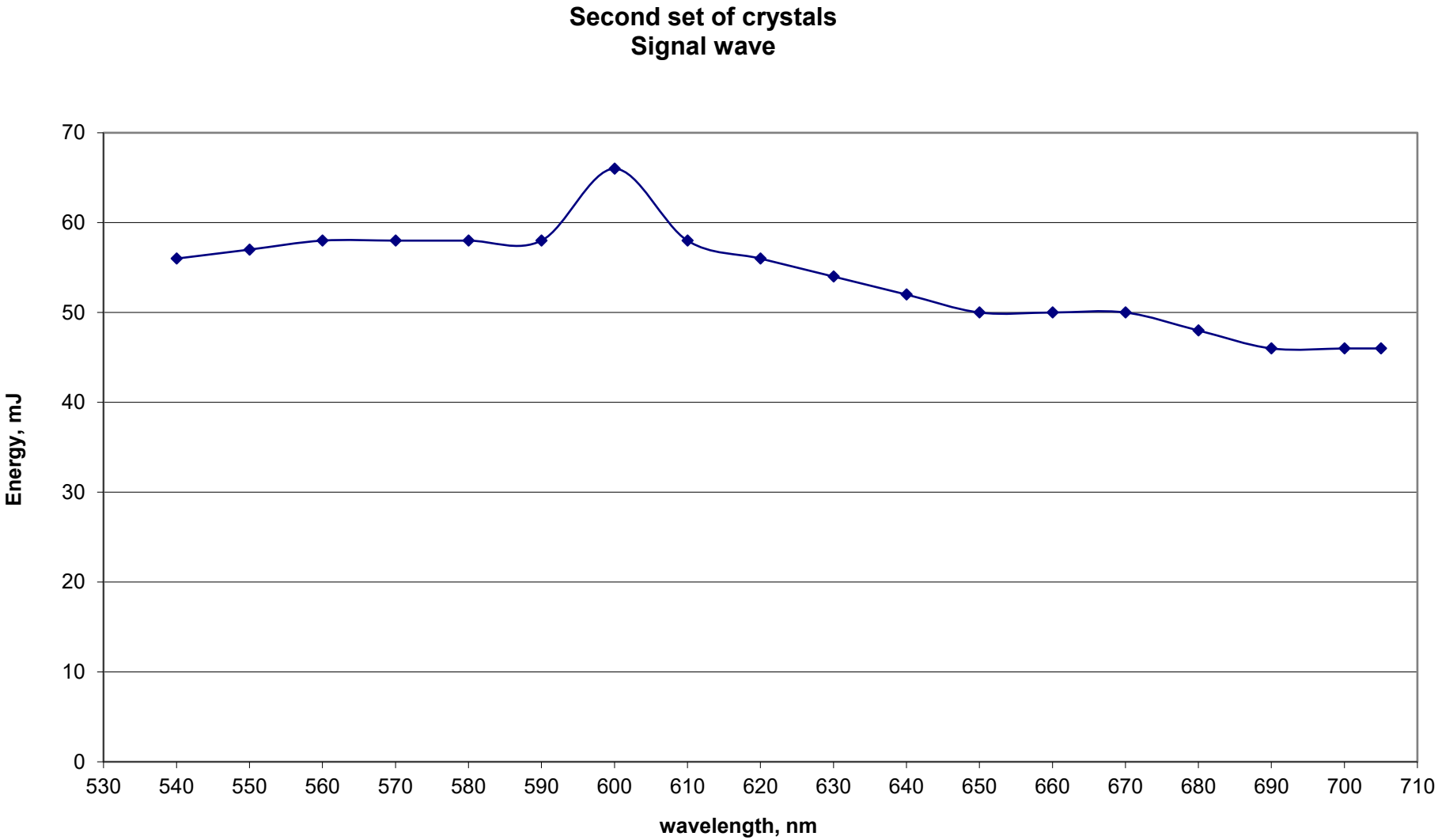

Figure 5.14 – Graph of the output energy of the signal wave against the wavelength for the II set of crystals

6 SPECTRAL EQUIPMENT

This section briefly outlines the operating principles and rules of the SF-56 spectrophotometer manufactured by OKB Spektr-LOMO, and of the RF-5301PC spectrofluorimeter manufactured by Shimadzu.

6.1 SF-56 spectrophotometer

The spectrophotometer is designed to measure the directional transmission coefficients of substances in the spectral range of the near ultraviolet, the entire visible region, as well as of the near-infrared range (190–1100 nm).

6.1.1 Operation principle

The operation principle of the spectrophotometer (Fig. 6.1) is based on measuring the ratio of two light fluxes: the light flux passing through the test sample and the flux incident on the test sample. To improve the measurement accuracy, and to eliminate the influence of scattered light, the signal intensity is recorded when the light from the radiation source is blocked.

The transmittance coefficient of the test sample T in percent is calculated by the formula:

$T = (U_s – U_d) / (U_i – U_d) * 100\%$

where U_i is the voltage proportional to the light flux incident on the sample; U_s is the voltage proportional to the light flux passing through the sample; U_d is the voltage proportional to the dark current of the photorecording device block.

Thus, at each wavelength, the intensities are measured consecutively:

- “dark zone”, which is formed by the overlap of light in the light filters block,
- light from a lamp
- light that has passed through the sample.

6.1.2 Optical scheme

Two lamps are used as a light source to cover the entire working spectral range from 190 to 1100 nm. A deuterium lamp (DDS-30) is used to work in the ultraviolet spectrum region, and a halogen lamp (KGM 12-10) is used for the visible range and near IR. The lamps are changed automatically at a 380 nm wavelength using a flat mirror that changes its position. When there is no mirror, the light from the deuterium lamp enters the monochromator. By introducing a mirror, the radiation of this lamp is blocked, and the light from the halogen lamp is reflected and directed to the entrance slit of the monochromator.

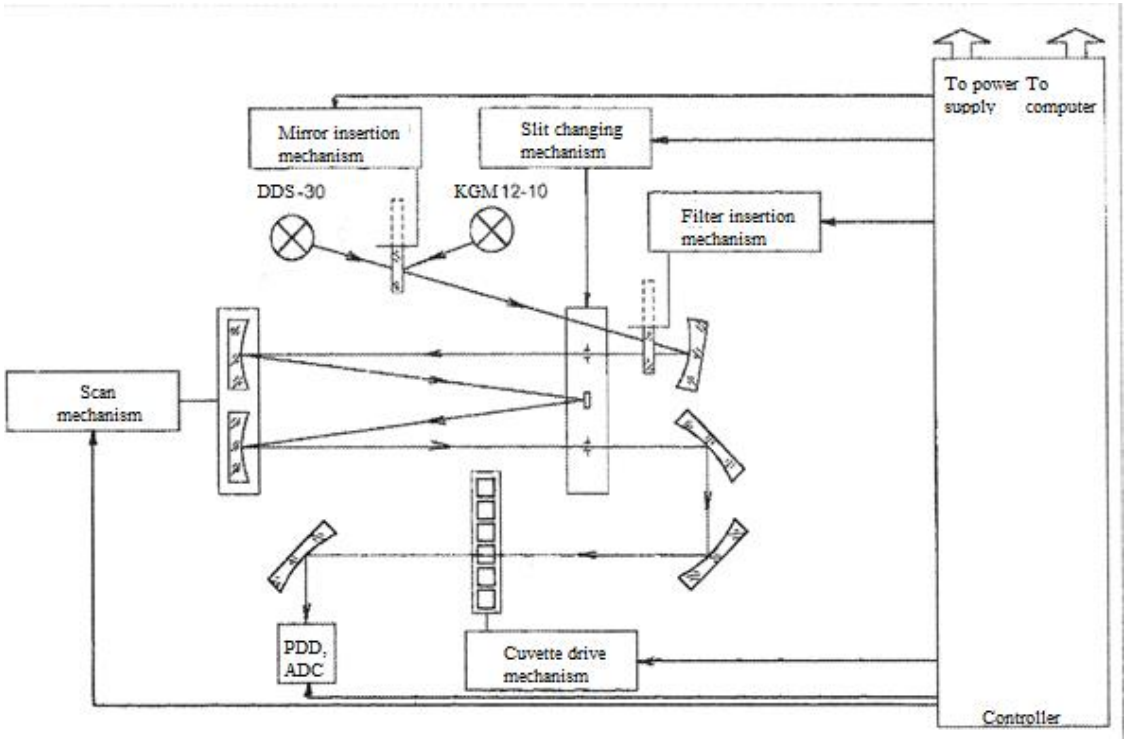

Figure 6.1 – Functional scheme of the SF-56 spectrophotometer

The monochromator consists of two concave diffraction gratings with a curvilinear stroke and variable pitch, and a spherical mirror, which acts as an intermediate slit. A system of toric mirrors forms a light beam that passes through the cell compartment, and the signal is recorded using a photodiode.

6.1.3 Operating procedure

1. Turn on the spectrophotometer pressing the green button on the power supply unit.

2. Run the SF-56 program from the desktop on the computer.

3. Select Device → Connect in the upper horizontal menu. The program will check the connection between the computer and the spectrophotometer and start the setup procedure, which includes the position correction of the monochromator diffraction gratings. In the visible range, the deuterium lamp has an intense narrow band at 656.1 nm; the correspondence of the gratings rotation angle to a certain wavelength is corrected accordingly. Stable operation of the spectrophotometer is ensured 30 min after it has been turned on, since this time is necessary to warm up the deuterium lamp.

4. Select the measurement mode in the upper horizontal menu. Point mode is designed to measure samples at discrete, user-specified wavelengths. Note that if it is necessary to make a large number of measurements at different wavelengths, or if the step between measurement points is constant (1, 5, 10 nm), then it is more convenient to use the "Scanning" mode, which measures spectra in the selected wavelength range (from 190 to 1100 nm).

5. Select the measured value in the main window of the program.

6.2 RF-5301PC spectrofluorimeter

The spectrofluorimeter irradiates the sample with excitation radiation and measures the signal emitted by the sample for a qualitative or quantitative analysis.

6.2.1 Operation principle

A typical instrument configuration is schematically shown in Fig. 6.2.

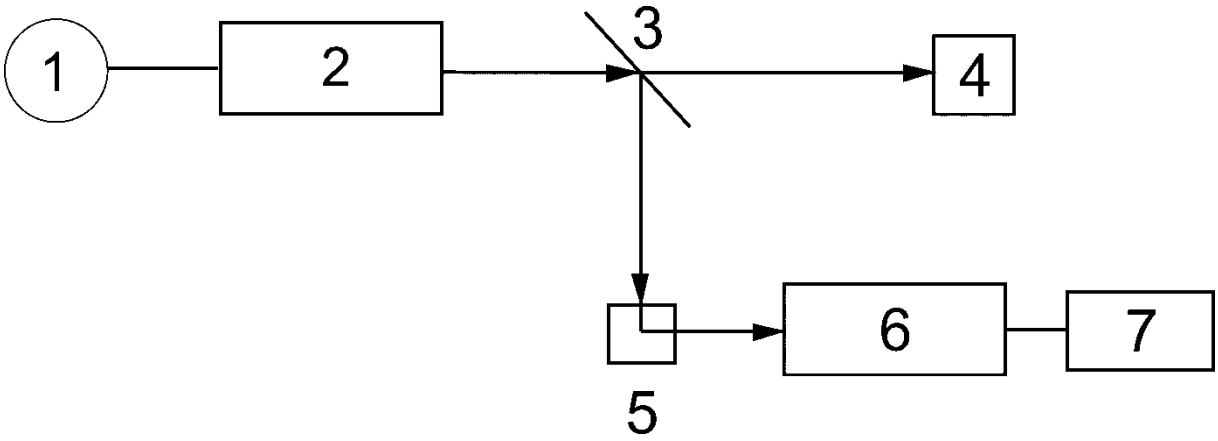

Figure 6.2 - Schematic diagram of the spectrofluorimeter: 1 - xenon lamp, 2 - excitation monochromator, 3 - beam splitter, 4 - PMT from the excitation side, 5 - sample in the cuvette compartment, 6 - emission monochromator, 7 - PMT from the emission side

A 150 W xenon lamp is used as the radiation source. The excitation monochromator extracts a predetermined wavelength range from the xenon lamp light to produce excitation radiation. Since brighter excitation light results in a higher spectrofluorimeter sensitivity, the excitation monochromator is equipped with a large aperture diffraction grating to collect as much light as possible.

The emission monochromator selectively receives the radiation of the sample, and its photomultiplier (PMT) measures the signal intensity. This monochromator has a diffraction grating of the same dimensions as that of the excitation monochromator for collecting as much light as possible.

The PMT on the excitation side is needed to correct the PMT signal on the emission side. Typically, xenon lamps used in spectrofluorimeters have a very high radiation intensity and a continuous emission spectrum. However, their tendency to emit unstable light can result in a higher noise if not taken care of. Besides, the non-identity of the xenon lamp emission spectrum and the spectral sensitivity of the PMT (these criteria are usually referred to as the instrumental function) causes spectrum distortion. To compensate for these factors, the photomultiplier on the excitation side receives part of the excitation light when scanning the signal, which corrects the resulting signal on the emission side PMT. Such a scheme is called a light source compensation system.

6.2.2 Operating procedure

1. Turn on the spectrofluorimeter using the switch on the right side of the instrument case. Check that the xenon lamp switch is also on.

2. Run the RF-5301PC program from the desktop on the computer. The program will check whether the computer is connected to the spectrofluorimeter and start the setup procedure, which includes checking monochromators and detectors. Stable operation of the spectrofluorimeter is ensured 30 minutes after it has been turned on, because this time is necessary to warm up the xenon lamp.

4. Select Configure - Parameters - Spectrum Parameters in the upper horizontal menu.

5. Select the parameters necessary for measuring the emission spectra in the window that appears:

Spectrum Type: Emission
EX Wavelength: 350 nm
Wavelength Range: 220 – 800
Sampling Interval: 1.0 nm
EX/ EM Slit Width: 5 nm / 5 nm

7 MAIN REQUIREMENTS FOR THE LABORATORY REPORT

The printed version of the report on laboratory work is presented to the lecturer in accordance with the requirements GOST 7.32-2017 "The research report. Structure and rules of presentation" (or ANSI/NISO Z39.18-2005 [4]). The report is defended by the student's presentation on the results of the work performed and their answers to the lecturer's questions.

The main structural elements of the report:

1) Title page (a sample design is shown in the next page).
2) The purpose of the work (based on the skills acquired during the work).
3) Brief theoretical information.
4) Laboratory part:
   a. equipment,
   b. optical scheme of the experiment,
   c. working process.
5) Experimental data:
   a. measurement results,
   b. formulas and calculations used,
   c. processing of received data.
6) Conclusions that reveal the analysis of the experimental data and the results obtained.

THE MINISTRY OF SCIENCE AND HIGHER EDUCATION
OF THE RUSSIAN FEDERATION

ITMO University
(ITMO)

L A B R E P O R T № _

for the course “Nonlinear Optics”

on the topic:

LAB TITLE

Student:
Group No. xxxx Surname Name

Teacher:
position, degree Surname Name

Saint Petersburg 2023

REFERENCES

1) Boyd B.W. Nonlinear Optics, 3rd Edition. – Elsevier. – 2008. – 640 p. – URL: http://www.fulviofrisone.com/attachments/article/404/Boyd%20Nonlinear%20Optics,%20Third%20Edition.pdf

2) Pavlov V.V., Semashko V.V. Optical parametric Generator (Opticheskii parametricheskii generator, in Russian) – Kazan Federal University. – 2014. – 68 p. – URL: https://kpfu.ru/portal/docs/F1427113584/Parametricheskie.generatory.sveta.pdf

3) Svelto O. Principles of Lasers, 5th ed. – Heidelberg, Springer – 2010. – 622 p. – URL: http://www.chemistry.uoc.gr/lapkin/OrazioSvelto_PrinciplesOfLasers_5thEd.pdf

4) ANSI/NISO Z39.18-2005 (R2010) Scientific and Technical Reports – Preparation, Presentation, and Preservation – 2010. – URL: https://www.niso.org/publications/z39.18-2005-r2010

Старовойтов Антон Андреевич
Матюшкина Анна Андреевна

Laboratory assignments for course «Nonlinear Optics»

Практикум

В авторской редакции
Иллюстрация на обложке: Дададжанов Далер Рауфович
Редакционно-издательский отдел Университета ИТМО
Зав. РИО Н.Ф. Гусарова
Подписано к печати
Заказ №
Тираж
Отпечатано на ризографе

Редакционно-издательский отдел
Университета ИТМО
197101, Санкт-Петербург, Кронверкский пр., 49, литер А